

Cross-linking of discotic tetraazaporphyrin dyes in 2 and 3 dimensions by “click” chemistry

Himadri Kayal,^a Mohamed M. Ahmida,^a Scott Dufour,^a Hi Taing,^a and S. Holger Eichhorn*^a

Supplementary Information

Content

Synthesis	p. 2-15
Mesomorphism	p. 17-30
Cross-Linking in solution and Col_h Mesophase	p. 31-33
Langmuir and Langmuir-Blodgett Films	p. 34

1 Synthesis

Chemicals: All reagents and solvents were purchased from Sigma-Aldrich and Fluka Chemical Companies and used as received unless otherwise stated. 1-Propanol and methanol were dried over 4 Å and 3 Å molecular sieves, respectively, whereas dry and air-free dichloromethane, tetrahydrofuran, and diethyl ether were obtained from a solvent purification system (Innovative Technology Inc. MA, USA, Pure-Solv 400). Silica gel 60 (35-70 mesh ASTM, from EM Science, Germany) was used for column chromatography and Silica Gel 60 aluminum backed sheets (EM Science, Germany) for thin layer chromatography.

Instrumentation: ^1H -NMR and ^{13}C -NMR spectra were obtained on Bruker NMR spectrometers (DRX 500 MHz and DPX 300 MHz). The residual proton signal of the deuterated solvent (usually chloroform (CDCl_3)) was used as a reference signal and multiplicities of the peaks are given as s = singlet, d = doublet, t = triplet, and m = multiplet. Coupling constants are given in Hz and only calculated for 1st-order systems. Data are presented in the following order: integration, multiplicity, and coupling constant. Fourier Transform Infrared spectra (FT-IR) were obtained on a Bruker Vector 22 as KBr pellets or thin films on KBr windows. Relative peak intensities and shapes in IR are abbreviated as vs = very strong, s = strong, m = medium, w = weak, and br = broad. Mass spectrometry measurements were performed by Kirk Green at the Regional Center for Mass Spectrometry (McMaster University) and Jiaxi Wang at the Mass Spectrometry and Proteomics Unit (Queen's University). UV/VIS absorption spectra were run on a Varian Cary 50 Conc UV-visible spectrophotometer. Elemental analysis was performed on a Perkin Elmer 2400 combustion CHNS analyser at the Centre for Catalysis and Materials Research at the University of Windsor.

1-Azido-3-bromo-propane 1a: (2.45 g, 60%); ^1H NMR (300 MHz, CDCl_3 , δ): 2.10 (2H, tt, $J^1 = 6.3$ Hz, $J^2 = 6.2$ Hz), 3.46 (2H, t, $J = 6.3$ Hz), 3.52 (2H, t, $J = 6.4$ Hz); IR (cm^{-1}): 2932 and 2856 (m, $\nu(\text{C-H})$), 2091 (s, $\nu(\text{N}_3)$); HRMS-Cl (m/z): calcd for $\text{C}_3\text{H}_6\text{BrN}_3$: 162.9745; Found: 162.9748 $[\text{M}]^+$.

1-Azido-6-bromo-hexane 1b: (3.08 g, 60%); ^1H NMR (300 MHz, CDCl_3 , δ): 1.44 (4H, m), 1.61 (2H, m), 1.86 (2H, m), 3.27 (2H, t, $J = 6.6$ Hz), 3.40 (2H, t, $J = 6.6$ Hz); IR (cm^{-1}): 2935 and 2871 ($\nu(\text{C-H})$), 2094 ($\nu(\text{N}_3)$); HRMS-Cl (m/z): calcd for $\text{C}_6\text{H}_{12}\text{BrN}$: 177.0153 $[\text{M} - \text{N}_2]$; Found: 177.0153 $[\text{M} - \text{N}_2]^+$.

1-Azido-9-bromononane 1c: (4.032 g, 65%); ^1H -NMR (300 MHz, CDCl_3 , δ): 1.30-1.41 (10H, m), 1.55-1.58 (2H, m), 1.84 (2H, tt, J^1 and $J^2 = 5.1$ Hz), 3.25 (2H, t, $J = 5.9$ Hz), 3.40 (2H, t, $J = 6.1$ Hz); ^{13}C -NMR (75 MHz, CDCl_3 , δ): 26.78, 28.21, 28.75, 28.92, 29.14, 29.37, 32.88, 34.12, 51.57; IR (cm^{-1}): 2936, 2870 ($\nu(\text{C-H})$), 2093 ($\nu(\text{N}_3)$); HRMS-Cl (m/z): calcd for $\text{C}_9\text{H}_{18}\text{BrN}$: 205.0592 $[\text{M} - \text{N}_2]$; Found: 205.0587 $[\text{M} - \text{N}_2]^+$.

*Synthesis of pent-4-yn-1-yl methanesulfonate 2a*¹

Methane sulfonyl chloride (1.87 mL, 2.750 g, 24 mmol) followed by triethyl amine (5 mL) were added dropwise to a stirred solution of 4-pentyne-1-ol (1.84 mL, 1.680 g, 20 mmol) in 50 mL of diethyl ether at 0 °C under nitrogen. The reaction mixture was stirred for 5 hrs at room temperature before quenched by the addition of deionized water. HCl_{aq} (1 M) was added dropwise to establish and maintain a pH of 7 and the product was extracted with H_2CCl_2 (3 x 50 mL). The combined organic layers were washed with water (3 x 50 mL), dried over anhydrous MgSO_4 , and concentrated in vacuum. Solid phase extraction from silica gel with H_2CCl_2 gave the pure product as a viscous brown liquid.

(2.9 g, 90%); ^1H -NMR (300 MHz, CDCl_3 , δ): 1.97 (2H, tt appears as p, $J = 6.6$ Hz), 2.02 (1H, t, $J = 2.7$), 2.37 (2H, dt, $J^d = 2.7$ Hz, $J^t = 6.9$ Hz), 3.04 (3H, s), 4.37 (2H, t, $J = 6.3$ Hz).

Synthesis of (8-bromooct-1-ynyl)trimethylsilane (2b) and (11-bromoundec-1-ynyl)trimethylsilane (2c) (both as mixtures with their disubstituted 1,10-bis(trimethylsilyl)deca-1,9-diyne and 1,13-bis(trimethylsilyl)trideca-1,12-diyne, respectively).

$n\text{BuLi}$ in hexane (1.6 M, 7.65 mL, 12.24 mmol) was added dropwise over a period of 5 min to a stirred solution of trimethyl silyl acetylene (1.44 mL, 1 g, 10.2 mmol) in 100 mL of THF at -78 °C under nitrogen. The resulting solution was stirred at -78 °C for 45 min before a solution of 1,6-dibromohexane (1.07 mL, 1.7 g, 6.8 mmol) or 1,9-dibromononane (1.3 mL, 1.94 g, 6.8 mmol) in hexamethyl phosphoramidate (1.2 mL, 1.219 g, 6.8 mmol) was added dropwise at -78 °C. The mixture was stirred at room temperature for 5 hrs and then poured into 250 mL of water and extracted with H_2CCl_2 (3 x 100 mL). The combined

¹ Bundy, G. L.; Lin, C. H.; Sih, J. C. *Tetrahedron* **1981**, 37, 4419.

organic layers were dried over anhydrous MgSO_4 , concentrated, and finally passed through a short column of silica gel with hexane as eluent. The products were obtained as 4:1 mixtures of mono- and di-acetylenes based on ^1H -NMR analysis and used for the next step without separation because only the mono-acetylene derivatives **2b** and **2c** will react and chromatographic removal of the di-acetylene derivatives from the reaction products **5b** and **5c** was straightforward.

(Mixture of **2b** with 1,10-bis(trimethylsilyl)deca-1,9-diyne: 1.260 g, 70%); ^1H NMR of **2b** (300 MHz, CDCl_3 , δ): 0.12 (9H, s), 1.36-1.47 (6H, m), 1.86-1.88 (2H, m), 2.21 (2H, t), 3.39 (2H, t, $J = 6.9$ Hz); ^{13}C NMR of mixture (75 MHz, CDCl_3 , δ): 3.28, 18.43, 19.87, 27.40, 27.73, 27.95, 28.32, 28.44, 28.55, 32.61, 32.72, 33.76, 33.92, 84.47, 84.66, 107.42, 107.66.

(Mixture of **2c** with 1,13-bis(trimethylsilyl)trideca-1,12-diyne: 1.498 g, 72%); ^1H NMR of **2c** (300 MHz, CDCl_3 , δ): 0.10 (9H, s), 1.30-1.39 (10H, m), 1.50 (2H, m), 1.85 (2H, m, $J = 6.9$ Hz), 3.40 (2H, t, $J = 6.9$ Hz); ^{13}C NMR of mixture (75 MHz, CDCl_3 , δ): 3.34, 18.68, 19.60, 26.15, 28.18, 28.51, 28.74, 29.01, 29.06, 29.30, 29.36, 29.46, 29.68, 32.86, 33.98, 84.42, 84.79, 107.40, 107.73.

Synthesis of 1,2-dicyano-1,2-bis(azido-alkylthio)ethylene 4a-c

Compound **1a** (2.445 g, 15 mmol) or **1b** (3.09 g, 15 mmol) or **1c** (3.72 g, 15 mmol) was added to a stirred solution of maleodinitrile **3** (1.3 g, 7 mmol) and NaI (105 mg, 0.7 mmol) in 50 mL of methanol at room temperature under nitrogen and the solution was stirred for 24 hrs. Methanol was evaporated under vacuum and the residue was extracted with H_2CCl_2 (3 x 50 mL). The combined organic layers were concentrated under vacuum and passed through a short column of silica gel using a 1:1 mixture of H_2CCl_2 /hexane as eluent to generate the pure products as viscous orange liquids.

cis-1,2-dicyano-1,2-bis(3-azido-propylthio)ethylene **4a**: (1.51 g, 70%); ^1H NMR (300 MHz, CDCl_3 , δ): 1.99 (4H, tt appears as p, $J = 6.74$ Hz), 3.21 (4H, t, $J = 7.07$ Hz), 3.48 (4H, t, $J = 6.34$ Hz); ^{13}C NMR (300 MHz, CDCl_3 , δ): 29.11, 32.02, 49.39, 111.82, 121.15; IR (cm^{-1}): 2928, 2855 (m, $\nu(\text{C-H})$), 2251 (m, $\nu(\text{CN})$), 2095 (s, $\nu(\text{N}_3)$), 1647 (m, $\nu(\text{C=C})$); HRMS-Cl (m/z): calcd for $\text{C}_{10}\text{H}_{12}\text{N}_8\text{S}_2$: 308.0626; Found: 308.0626 $[\text{M}]^+$.

cis-1,2-dicyano-1,2-bis(6-azido-hexylthio)ethylene **4b**: (1.92 g, 65%); ^1H NMR (300 MHz, CDCl_3 , δ): 1.36 (8H, m), 1.53 (4H, m), 1.67 (4H, m), 3.05 (4H, t, $J = 7.2$ Hz), 3.20 (4H, t, $J = 6.9$ Hz); ^{13}C NMR (75 MHz, CDCl_3 , δ): 27.49, 27.55, 28.81, 29.57, 34.69, 51.26, 112.05, 120.24; IR (cm^{-1}): 2928, 2855 (m, $\nu(\text{C-H})$), 2259 (m, $\nu(\text{CN})$), 2095 (s, $\nu(\text{N}_3)$), 1643 (m, $\nu(\text{C=C})$); HRMS-Cl (m/z): calcd for $\text{C}_{16}\text{H}_{24}\text{N}_8\text{S}_2$: 392.1561; Found: 392.1565 $[\text{M}]^+$.

cis-1,2-dicyano-1,2-bis(9-azido-nonylthio)ethylene **4c**: (2.068 g, 62%); ^1H -NMR (300 MHz, CDCl_3 , δ): 3.29 (4H, t, $J = 6.9$ Hz), 3.14 (4H, t, $J = 7.5$ Hz), 1.75 (4H, m), 1.35- 1.48 (24H, m); ^{13}C -NMR (75 MHz, CDCl_3 , δ):

26.76, 28.88, 29.01, 29.20, 29.31, 29.49, 30.59, 35.37, 51.50, 140.71, 153.22; IR (cm⁻¹): 2926, 2855 (m, ν (C-H)), 2256 (m, ν (CN)), 2096 (s, ν (N₃)), 1642 (m, ν (C=C)); HRMS-Cl (m/z): calcd for C₂₂H₃₆N₈S₂: 476.2504; Found: 476.2516 [M]⁺.

Synthesis of cis-1,2-dicyano-1,2-bis(pent-4-ynyl-1-thio)ethylene 5a

Pent-4-yn-1-yl methanesulfonate **2a** (2.6 g, 16 mmol) was added to a stirred solution of maleodinitrile **3** (1.3 g, 7 mmol) in 50 mL anhydrous methanol at room temperature and stirred for 24 hrs under nitrogen. MeOH was evaporated under vacuum and the residue was extracted with H₂CCl₂ (3 x 50 mL). The combined organic layers were concentrated under vacuum and passed through a column of silica gel with H₂CCl₂/hexanes 1:1 as eluent to generate the pure product as a viscous orange liquid.

(1.25 g, 65 %); ¹H NMR (300 MHz, CDCl₃, δ): 1.95 (4H, m), 2.02 (2H, t, J = 2.8 Hz), 2.37 (4H, dt, J^1 = 2.9 Hz, J^2 = 6.7 Hz), 3.26 (4H, t, J = 6.0 Hz); ¹³C-NMR (75 MHz, CDCl₃, δ): 17.20, 28.44, 33.70, 70.18, 81.95, 111.95, 121.26; HRMS-Cl (m/z): calcd for C₁₄H₁₄N₂S₂: 274.0598; Found: 274.0591 [M]⁺.

Synthesis of cis-1,2-dicyano-1,2-bis(oct-7-ynyl-1-thio)ethylene 5b and cis-1,2-dicyano-1,2-bis(undec-10-ynyl-1-thio)ethylene 5c

A mixture of (8-bromooct-1-yn-1-yl)trimethylsilane **2b** (contains about 20 mol% 1,10-bis(trimethylsilyl)deca-1,9-diyne) (1.191 g of mixture, about 3.6 mmol of **2b**) or (11-bromoundec-1-ynyl)trimethylsilane **2c** (contains about 20 mol% 1,13-bis(trimethylsilyl)trideca-1,11-diyne) (1.399 g of mixture, about 3.6 mmol of **2c**) with K₂CO₃ (1.105 g, 8 mmol) in 100 mL of MeOH was stirred at room temperature for 5 hrs to remove the trimethylsilane groups. Excess of K₂CO₃ was precipitated at 0 °C and filtered off before a solution of maleodinitrile **3** (280 mg, 1.5 mmol) and NaI (24 mg, 0.15 mmol) in 20 mL of MeOH was added. The reaction mixture was stirred for 24 hrs at room temperature, MeOH was evaporated, and the residue was suspended in 100 mL of H₂CCl₂. Precipitates were removed by filtration and the filtrate was concentrated for column chromatography on silica gel with H₂CCl₂/hexane 4:1 as eluent to generate the pure products **5b** and **5c** as viscous yellow liquids.

cis-1,2-dicyano-1,2-bis(oct-7-ynyl-1-thio)ethylene 5b

(774 mg, 60%) ¹H NMR (300 MHz, CDCl₃, δ): 1.47-1.46 (12H, m), 1.74 (4H, m), 1.94 (2H, t, J = 2.7 Hz), 2.19 (4H, dt, J^1 = 2.6 Hz and J^2 = 6.9 Hz), 3.12 (4H, t, J = 7.2 Hz); ¹³C-NMR (75 MHz, CDCl₃, δ): 18.38, 28.01, 28.11, 28.21, 29.83, 35.08, 68.56, 84.39, 112.18, 121.12; HRMS-Cl (m/z): calcd for C₂₀H₂₈N₂S₂: 358.1537; Found: 358.1543 [M]⁺.

cis-1,2-dicyano-1,2-bis(undec-10-ynyl-1-thio)ethylene 5c

(957 mg, 61%) ^1H NMR (300 MHz, CDCl_3 , δ): 3.14 (t, $J = 7.2$ Hz, 4H), 2.12 (dt, $J^1 = 2.5$ Hz and $J^2 = 6.9$ Hz, 4H), 1.97 (t, $J = 2.4$ Hz, 2H), 1.75 (m, 4H), 1.29-1.45 (m, 24H); ^{13}C -NMR (75 MHz, CDCl_3 , δ): 121.05, 112.15, 84.75, 68.28, 35.11, 29.88, 29.76, 29.27, 29.00, 28.95, 28.70, 28.46, 18.43; HRMS-Cl (m/z): calcd for $\text{C}_{26}\text{H}_{40}\text{N}_2\text{S}_2$: 442.2476; Found: 442.2485 $[\text{M}]^+$.

Synthesis of octa-azide and octa-acetylene TAPs (6a-c and 7a-c)

Mg powder (24.6 mg, 1 mmol) and 5 mg of iodine crystals were refluxed overnight in 50 mL of dry propan-1-ol under nitrogen until all Mg is reacted to Mg(II) propanolate. Maleodinitrile **4a** (1.54 g, 5 mmol) (or **4b** (1.96 g, 5 mmol), **4c** (2.38 g, 5 mmol), **5a** (1.372 g, 5 mmol), **5b** (1.793 g, 5 mmol), **5c** (2.21 g, 5 mmol)) was added and the suspension was heated at reflux for 24 hrs. The resulting greenish-blue suspension was cooled to room temperature, diluted with 50 mL of water, filtered, and the filter residue was washed with methanol/water 1:1 until the filtrate remains colourless. The filter residue was dissolved in a mixture of 50 mL acetic acid and 10 mL THF and stirred at 80 °C for about 8 hours until demetallation was completed. Progress of the demetallation was monitored by UV-Vis spectroscopy. Water (100 mL) was added to the now purple solution and the product was extracted with H_2CCl_2 (3 x 100 mL). The combined H_2CCl_2 layers were dried over anhydrous MgSO_4 and the solvent was removed under vacuum to give the crude TAP. Precipitation of the crude TAP from acetone solution by slow addition of a 2:1 mixture of methanol and water purifies the TAPs to about 90% purity and these samples were further purified by flash chromatography on silica gel with H_2CCl_2 /hexane 1:2 as eluent. The purified metal-free TAPs were obtained as dark purple solids.

2,3,7,8,12,13,17,18-octakis(azidopropylthio)-5,10,15,20-tetraazaporphyrin (6a) (839 mg, 68%): ^1H NMR (300 MHz, CDCl_3 , δ): -1.45 (2H, s, NH), 2.18 (16H, m, broad), 3.67 (16H, m, broad), 4.19 (16H, m, broad); ^{13}C NMR (75, MHz, CDCl_3 , δ): 29.21, 34.42, 49.21, 139.82, 151 (not observed); IR (cm^{-1}): 3290 (m, ν (N-H)), 2930 (m, ν (C-H)), 2098 (s, ν (N_3)); UV/VIS in THF (λ_{max} in nm, ϵ in $\text{dm}^3 \text{mol}^{-1} \text{cm}^{-1}$): 344 (44300), 513 (20600), 651 (26100), 712 (34200); EA calcd for $\text{C}_{40}\text{H}_{50}\text{N}_{32}\text{S}_8$: 38.88 %C, 36.28 %N, 4.08 %H; Found: 39.12 %C, 36.00 %N, 4.15 %H.

2,3,7,8,12,13,17,18-octakis(azidohexylthio)-5,10,15,20-tetraazaporphyrin (6b) (1.098 g, 70%): ^1H NMR (300 MHz, CDCl_3 , δ): -1.12 (2H, s, NH), 1.31-1.45 (16H, m), 1.47-1.71 (32H, m), 1.88 (16H, t, $J = 6.9$ Hz), 3.19 (16H, t, $J = 6.6$ Hz), 4.09 (16H, t, $J = 6.9$ Hz); ^{13}C NMR (75 MHz, CDCl_3 , δ): 26.12, 28.63, 28.81, 29.72, 34.89, 49.86, 138.01, 149.93; IR (cm^{-1}): 3285 (m, ν (N-H), inner core NH), 2932 (m, ν (C-H), CH_2), 2095 (s, ν (N_3)); UV/VIS in THF (λ_{max} in nm, ϵ in $\text{dm}^3 \text{mol}^{-1} \text{cm}^{-1}$): 342 (44100), 515 (20500), 655 (26200), 714 (34200); EA calcd for $\text{C}_{64}\text{H}_{98}\text{N}_{32}\text{S}_8$: 48.89 %C, 28.51 %N, 6.28 %H; Found: 48.80 %C, 28.30 %N, 6.44 %H.

2,3,7,8,12,13,17,18-octakis(azidononylthio)-5,10,15,20-tetraazaporphyrin (**6c**) (1.259 g, 66%): ^1H NMR (300 MHz, CDCl_3 , δ): -1.06 (2H, s, NH), 1.28 (64H, m), 1.59 (32H, m), 1.97 (16H, m), 3.20 (16H, broad), 4.12 (16H, broad); ^{13}C NMR (75 MHz, CDCl_3 , δ): 26.71, 28.84, 28.96, 29.15, 29.26, 29.44, 30.54, 35.32, 51.45, 140.63, 153.43; IR (cm^{-1}): 3283 (m, $\nu(\text{N-H})$), 2920 (m, $\nu(\text{C-H})$), 2100 (s, $\nu(\text{N}_3)$); UV/VIS in THF (λ_{max} in nm, ϵ in $\text{dm}^3 \text{mol}^{-1} \text{cm}^{-1}$): 344 (44 300), 510 (21 000), 651 (25 900), 713 (34115); HRMS-MALDI (m/z): calcd for $\text{C}_{88}\text{H}_{146}\text{N}_{32}\text{S}_8+\text{H}$: 1908.0252; Found: 1908.0242 $[\text{M}+\text{H}]^+$; EA calcd for $\text{C}_{88}\text{H}_{146}\text{N}_{32}\text{S}_8$: 55.37 %C, 23.48 %N, 7.71 %H; Found: 55.25 %C, 23.31 %N, 7.84 %H.

2,3,7,8,12,13,17,18-octakis(pent-4-yn-1-ylthio)-5,10,15,20-tetraazaporphyrin (**7a**) (770 mg, 70%): ^1H NMR (300 MHz, CDCl_3 , δ): -1.30 (2H, s, NH), 1.90 (8H, s), 2.08 (16H, tt appears as p, $J = 6.9$ Hz), 2.52 (16H, t, $J = 2.1$ Hz), 4.18 (16H, t, $J = 7.2$ Hz); ^{13}C NMR (75 MHz, CDCl_3 , δ): 17.72, 29.28, 34.00, 69.33, 83.43, 140.59, 153.35; IR (cm^{-1}): 3290 (s, $\nu(\text{C-H})$ alkyne and w, $\nu(\text{N-H})$), 2917, 2850 (m, $\nu(\text{C-H})$, CH_2), 2115 (w, $\nu(\text{C}\equiv\text{C})$); UV/VIS in THF (λ_{max} in nm, ϵ in $\text{dm}^3 \text{mol}^{-1} \text{cm}^{-1}$): 355 (43090), 565 (18940), 645 (26470), 710 (34200); HRMS-MALDI (m/z): calcd for $\text{C}_{56}\text{H}_{58}\text{N}_8\text{S}_8+\text{H}$: 1099.2625; Found: 1099.2646 $[\text{M}+\text{H}]^+$.

2,3,7,8,12,13,17,18-octakis(oct-7-yn-1-ylthio)-5,10,15,20-tetraazaporphyrin (**7b**) (976 mg, 68%): ^1H NMR (300 MHz, CDCl_3 , δ): -1.13 (2H, s, NH), 1.38-1.72 (48H, m), 1.79-1.96 (24H, m), 2.04-2.19 (16H, m), 4.08 (16H, t, $J = 7.2$ Hz); ^{13}C NMR (75 MHz, CDCl_3 , δ): 18.37, 28.39, 28.45, 29.75, 30.41, 35.24, 68.26, 84.49, 140.63, 153.2; IR (cm^{-1}): 3290 (s, $\nu(\text{C-H})$ alkyne and w, $\nu(\text{N-H})$), 2930, 2854 (m, $\nu(\text{C-H})$, CH_2), 2115 (w, $\nu(\text{C}\equiv\text{C})$); UV/VIS in THF (λ_{max} in nm, ϵ in $\text{dm}^3 \text{mol}^{-1} \text{cm}^{-1}$): 355 (43030), 562 (19091), 642 (26060), 710 (33333); HRMS-MALDI (m/z): calcd for $\text{C}_{80}\text{H}_{106}\text{N}_8\text{S}_8+\text{H}$: 1435.6384; Found: 1435.6380 $[\text{M}+\text{H}]^+$.

2,3,7,8,12,13,17,18-octakis(undeca-10-yn-1-ylthio)-5,10,15,20-tetraazaporphyrin (**7c**) (1.241 g, 70%): ^1H NMR (300 MHz, CDCl_3 , δ): -1.09 (2H, s, NH), 1.2-1.3 (64H, m), 1.42 (16H, m), 1.60 (16H, m), 1.89 (24H, broad), 2.10 (16H, broad), 4.10 (16H, broad); ^{13}C NMR (75 MHz, CDCl_3 , δ): 18.33, 28.40, 28.68, 28.78, 28.90, 29.04, 29.26, 30.49, 35.28, 68.05, 84.65, 140.42 (HMBC at 130 MHz), 151 (not observed); IR (cm^{-1}): 3300 (s, $\nu(\text{C-H})$ alkyne and w, $\nu(\text{N-H})$), 2933, 2845 (m, $\nu(\text{C-H})$, CH_2), 2113 (w, $\nu(\text{C}\equiv\text{C})$); UV/VIS in THF (λ_{max} in nm, ϵ in $\text{dm}^3 \text{mol}^{-1} \text{cm}^{-1}$): 360 (43100), 565 (18965), 645 (26500), 712 (34200); EA calcd for $\text{C}_{104}\text{H}_{154}\text{N}_8\text{S}_8$: 70.46 %C, 6.32 %N, 8.76 %H; Found: 70.19 %C, 6.15 %N, 8.91 %H.

Synthesis of octa-azide and octa-acetylene copper TAPs (**6a-cCu** and **7a-cCu**)

Metal-free TAP **6a** (617 mg, 0.5 mmol) (or **6b** (785 mg, 0.5 mmol), **6c** (954 mg, 0.5 mmol), **7a** (550 mg, 0.5 mmol), **7b** (718 mg, 0.5 mmol), **7c** (886 mg, 0.5 mmol)) was stirred in a solution of copper(II) acetylacetonate (262 mg, 1.0 mmol) in THF (50 mL) at 60 °C for 6-8 hrs. Progress and completion of the metallation with copper(II) was monitored by UV-VIS spectroscopy. Ethyl acetate (100 mL) was added

and the mixture was then extracted with an aqueous solution of ammonium chloride (5% w/w, 3 x 100 mL) and finally with water (2 x 100 mL). The organic layer was dried over anhydrous MgSO₄, concentrated, and filtered through a small amount of silica gel with ethyl acetate/hexane 1:3 to generate the purified copper TAPs as dark blue solids.

2,3,7,8,12,13,17,18-octakis(azidopropylthio)-5,10,15,20-tetraazaporphyrinato-copper (6aCu) (571 mg, 88%); IR (cm⁻¹): 2917, 2849 (m, ν(C-H), CH₂), 2093 (s, ν(N₃), azide); UV/VIS in THF (λ_{max} in nm, ε in dm³ mol⁻¹ cm⁻¹): 362 (21820), 500 (7576), 667 (30606); EA calcd for C₄₀H₄₈CuN₃₂S₈: 37.04 %C, 34.56 %N, 3.73 %H; Found: 36.79 %C, 34.35 %N, 3.91 %H.

2,3,7,8,12,13,17,18-octakis(azidohexylthio)-5,10,15,20-tetraazaporphyrinato-copper (6bCu) (653 mg, 81%); MW: IR (cm⁻¹): 2929, 2853 (m, ν(C-H), CH₂), 2094 (s, ν(N₃), azide); UV/VIS in THF (λ_{max} in nm, ε in dm³ mol⁻¹ cm⁻¹): 365 (21970), 505 (7758), 670 (30667); HRMS-MALDI (*m/z*): calcd for C₆₄H₉₆CuN₃₂S₈+H: 1632.5635; Found: 1632.5630 [M+H]⁺.

2,3,7,8,12,13,17,18-octakis(azidononylthio)-5,10,15,20-tetraazaporphyrinato-copper(6cCu) (788 mg, 80%); IR (cm⁻¹): 2915, 2851 (m, ν(C-H), CH₂), 2090 (s, ν(N₃), azide); UV/VIS in THF (λ_{max} in nm, ε in dm³ mol⁻¹ cm⁻¹): 365 (24857), 504 (8354), 670 (30616); HRMS-MALDI (*m/z*): calcd for C₈₈H₁₄₄CuN₃₂S₈+H: 1968.9391; Found: 1968.9329 [M+H]⁺.

2,3,7,8,12,13,17,18-octakis(pent-4-yn-1-ylthio)-5,10,15,20-tetraazaporphyrinato-copper (7aCu) (493 mg, 85%); IR (cm⁻¹): 3353, 3295 (s, ν(C-H) alkyne), 2930, 2853 (s, ν(C-H), CH₂), 2116 (w, ν(C≡C)); UV/VIS in THF (λ_{max} in nm, ε in dm³ mol⁻¹ cm⁻¹): 360 (25151), 500 (8667), 665 (29090); HRMS-MALDI (*m/z*): calcd for C₅₆H₅₆CuN₈S₈+H: 1160.1767; Found: 1160.1754 [M+H]⁺.

2,3,7,8,12,13,17,18-octakis(oct-7-yn-1-ylthio)-5,10,15,20-tetraazaporphyrinato-copper (7bCu) (600 mg, 80%); IR (cm⁻¹): 3352, 3300 (s, ν(C-H) alkyne), 2930, 2853 (s, ν(C-H), CH₂), 2117 (w, ν(C≡C)); UV/VIS in THF (λ_{max} in nm, ε in dm³ mol⁻¹ cm⁻¹): 365 (24850), 503 (8364), 670 (30606); HRMS-MALDI (*m/z*): calcd for C₈₀H₁₀₄CuN₈S₈+H: 1496.5523; Found: 1496.5552 [M+H]⁺.

2,3,7,8,12,13,17,18-octakis(undeca-10-yn-1-ylthio)-5,10,15,20-tetraazaporphyrinato-copper(17cCu) (726 mg, 82%); IR (cm⁻¹): 3300, 3350 (s, ν(C-H) alkyne), 2928, 2850 (s, ν(C-H), CH₂), 2110 (w, ν(C≡C)); UV/VIS in THF (λ_{max} in nm, ε in dm³ mol⁻¹ cm⁻¹): 365 (21975), 505 (7760), 670 (30655); EA calcd for C₁₀₄H₁₅₂CuN₈S₈: 68.09 %C, 6.11 %N, 8.35 %H; Found: 67.83 %C, 5.99 %N, 8.42 %H.

NMR Spectra of Metal-Free TAPs

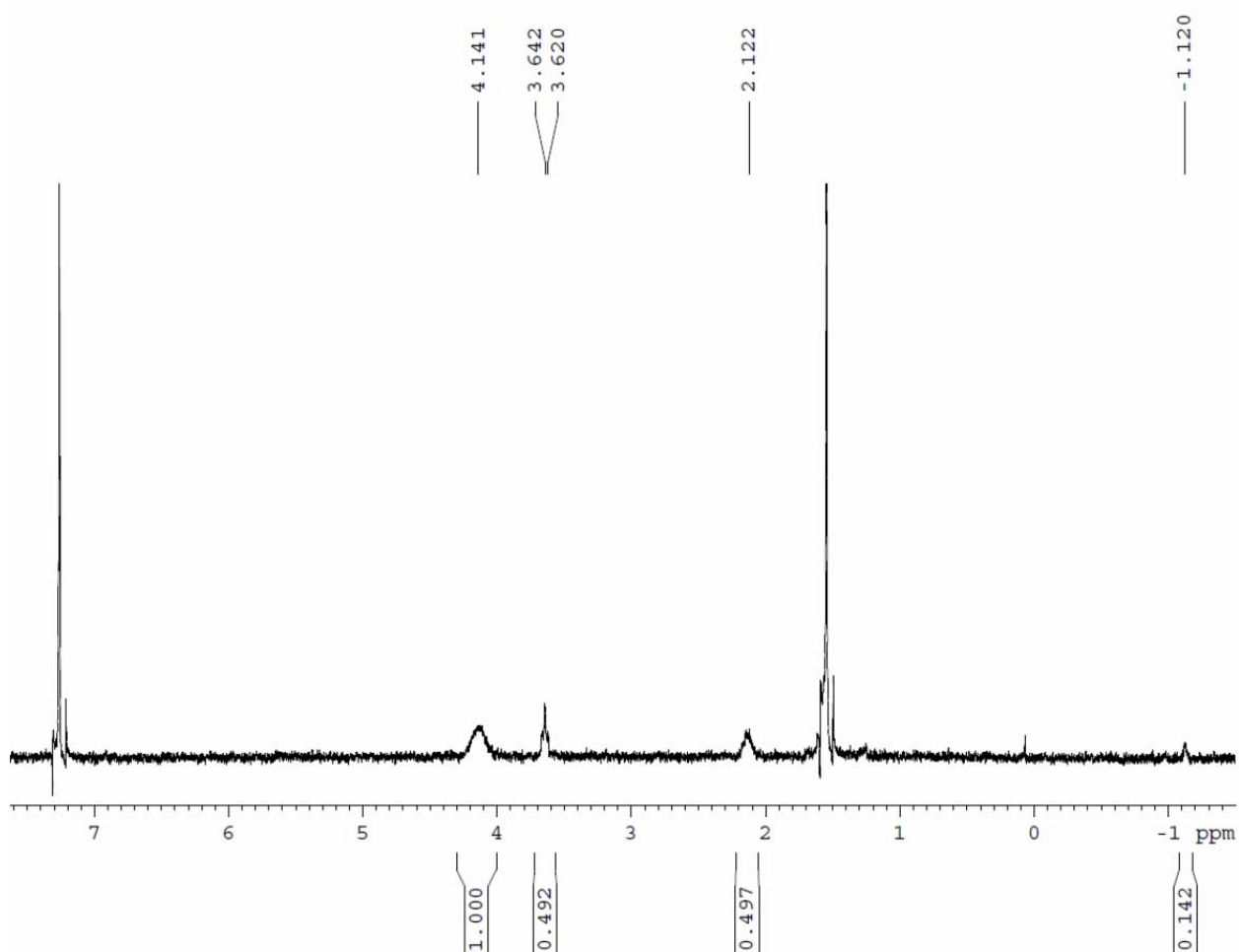


Figure S1: ^1H -NMR of **6a** in CDCl_3 . The absorption peaks are broadened do to aggregation. Measurements at 50 °C and at lower concentration did not significantly decrease line broadening but measurements at 100 °C or higher temperatures were not tested. Aggregation is also likely responsible for the too low integration values of the peaks at 3.6 and 2.1.

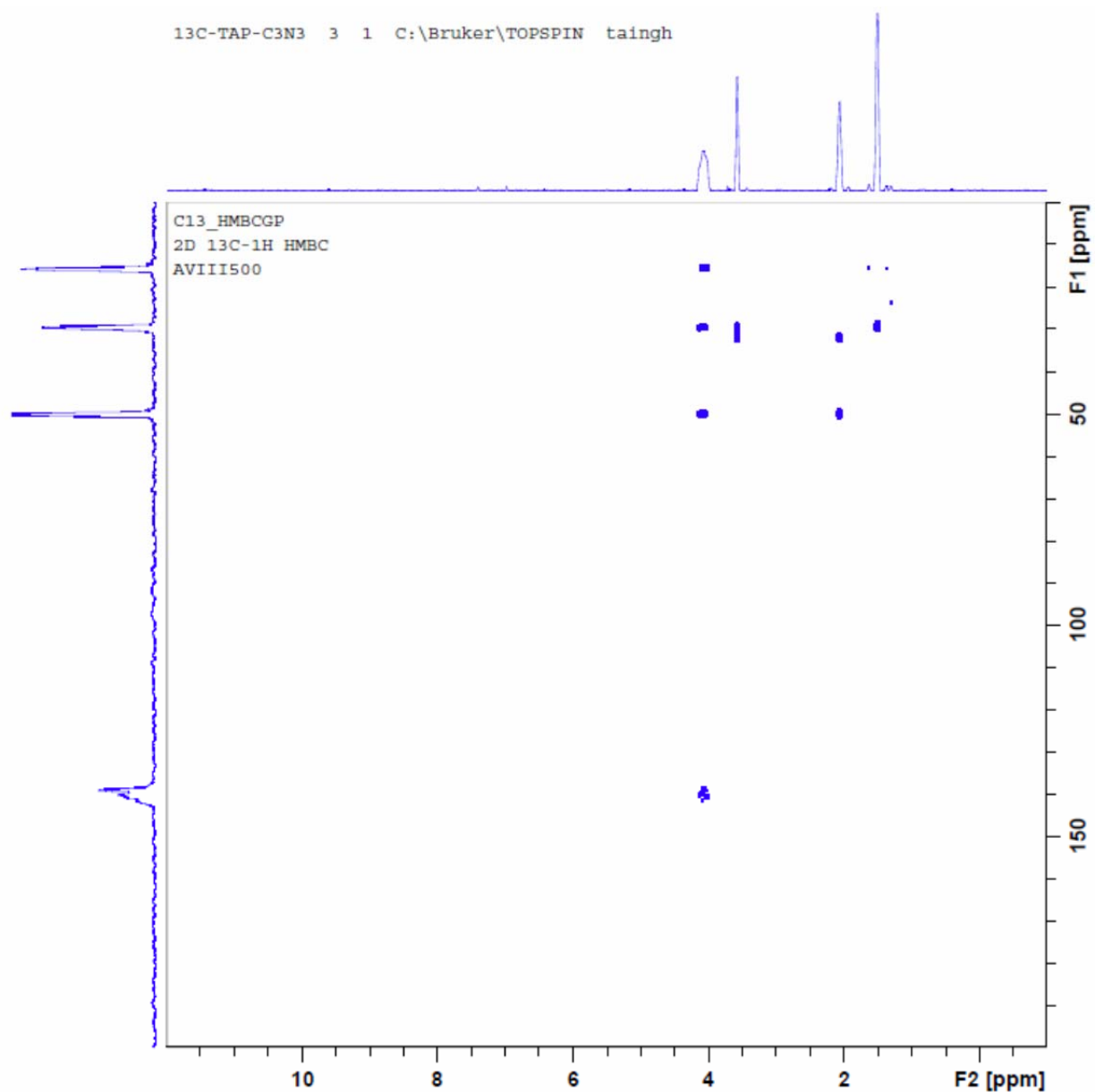


Figure S2: ^{13}C -NMR of **6a** in CDCl_3 did not resolve the two carbon signals of the TAP core after 36 hours of collection but HMBC improved the sensitivity of these carbons and at least the carbon atom at 140 ppm was visible. However, the presence of the TAP core is independently verified by UV-Vis spectroscopy. The peak at 1.5 ppm in the H-NMR part is water that appears to couple.

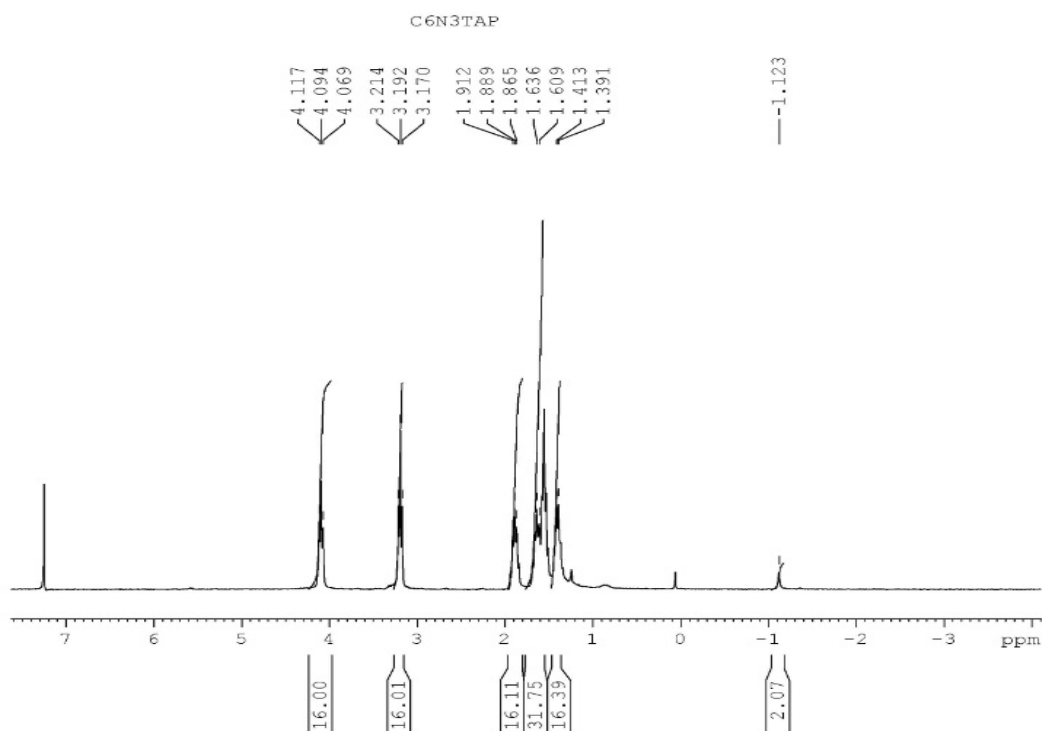


Figure S3: ^1H -NMR of **6b** in CDCl_3 .

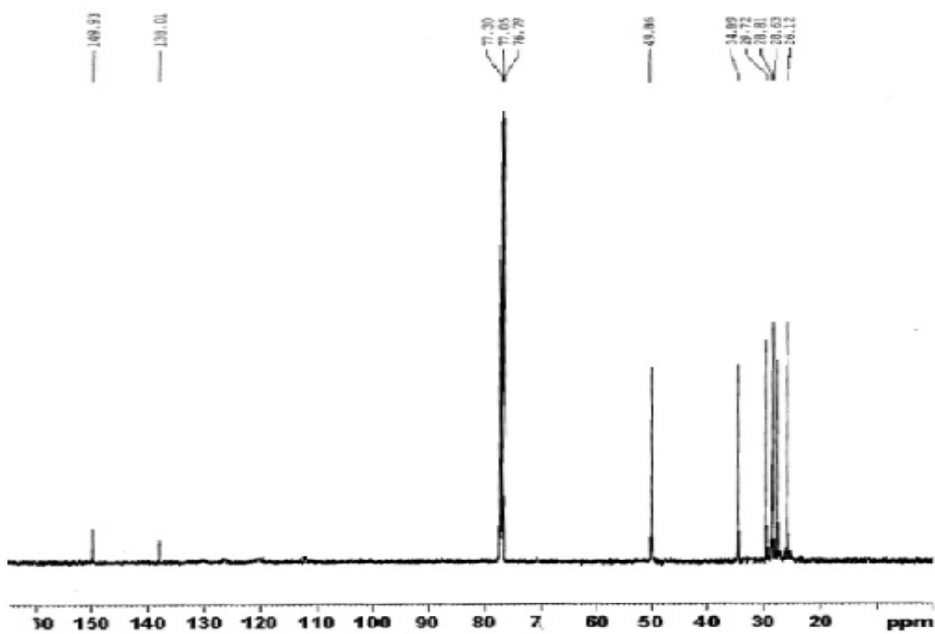


Figure S4: ^{13}C -NMR of **6b** in CDCl_3 .

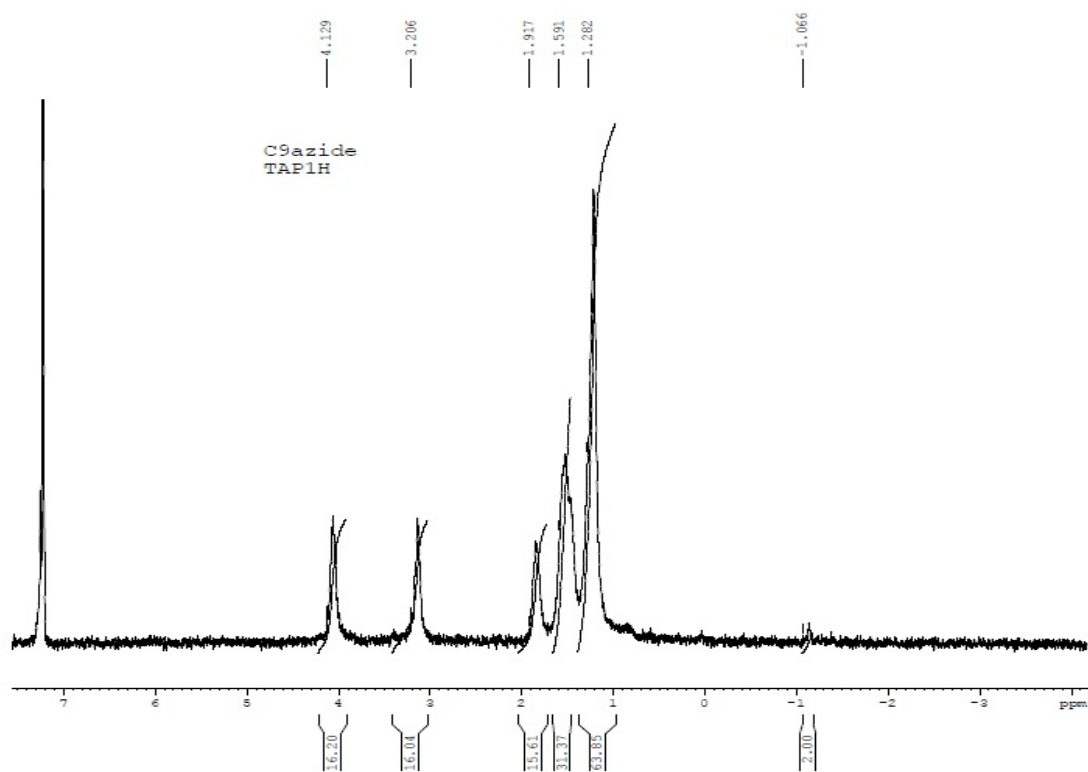


Figure S5: ^1H -NMR of **6c** in CDCl_3 .

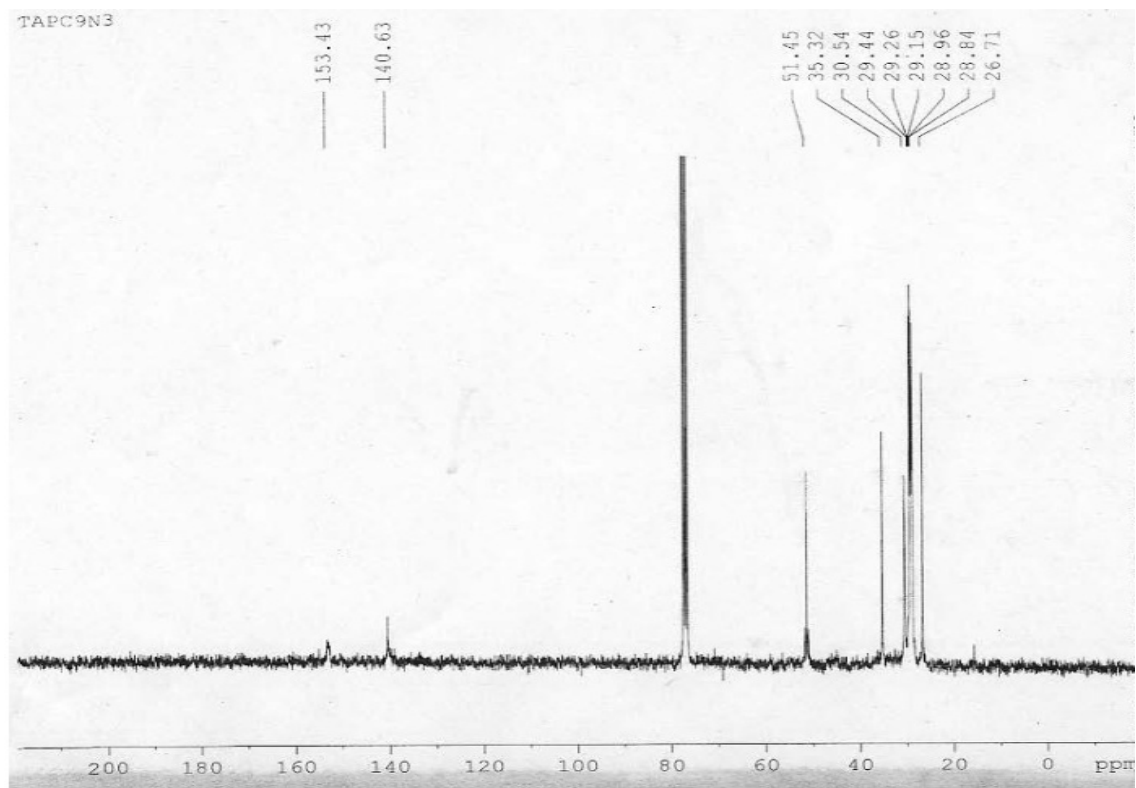


Figure S6: ^{13}C -NMR of **6c** in CDCl_3 .

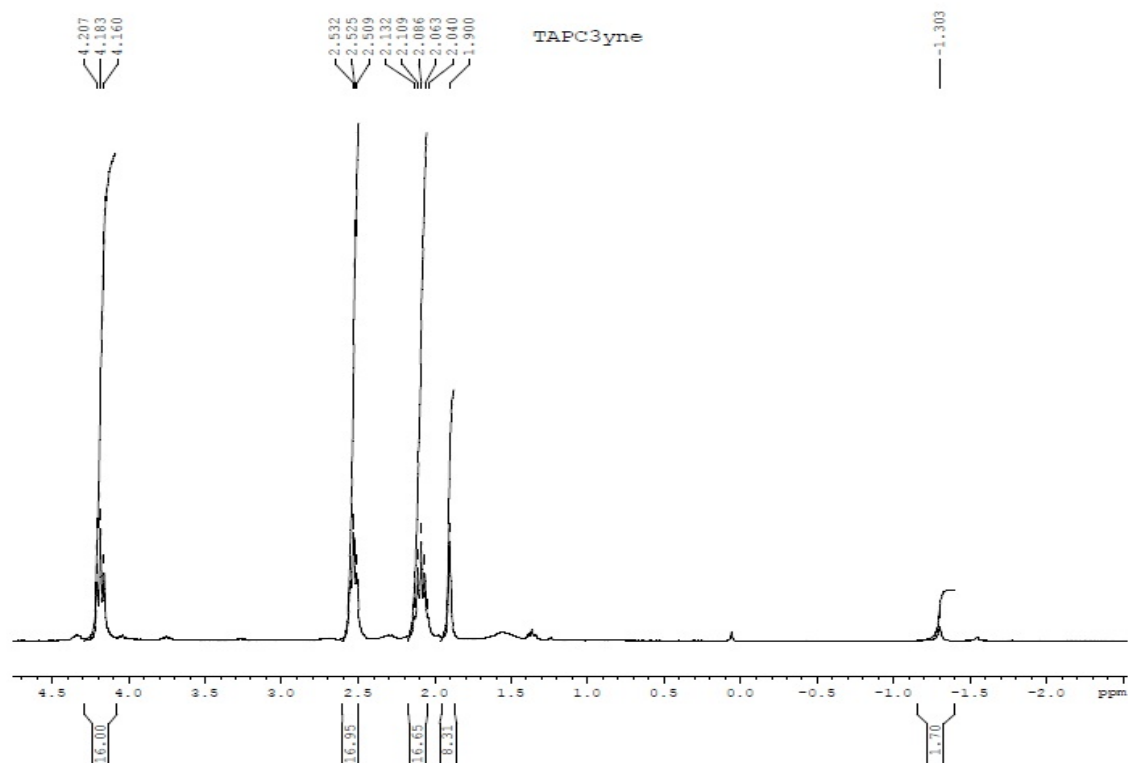


Figure S7: ^1H -NMR of **7a** in CDCl_3 .

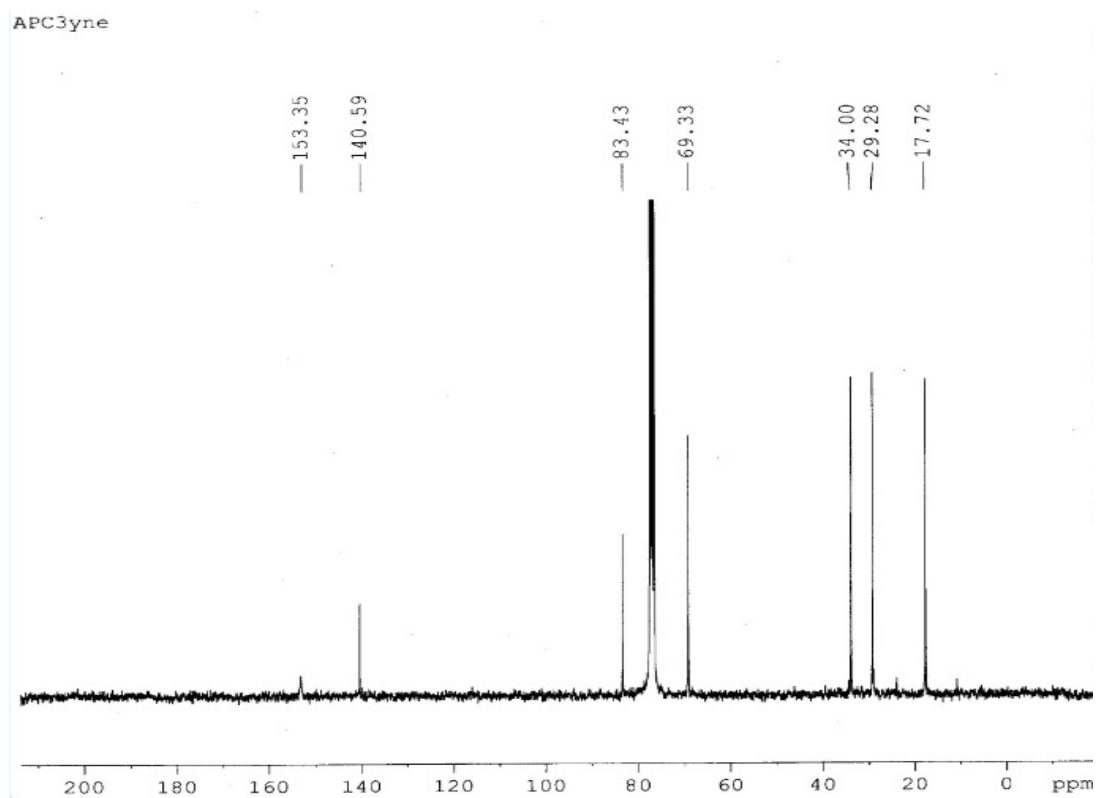


Figure S8: ^{13}C -NMR of **7a** in CDCl_3 .

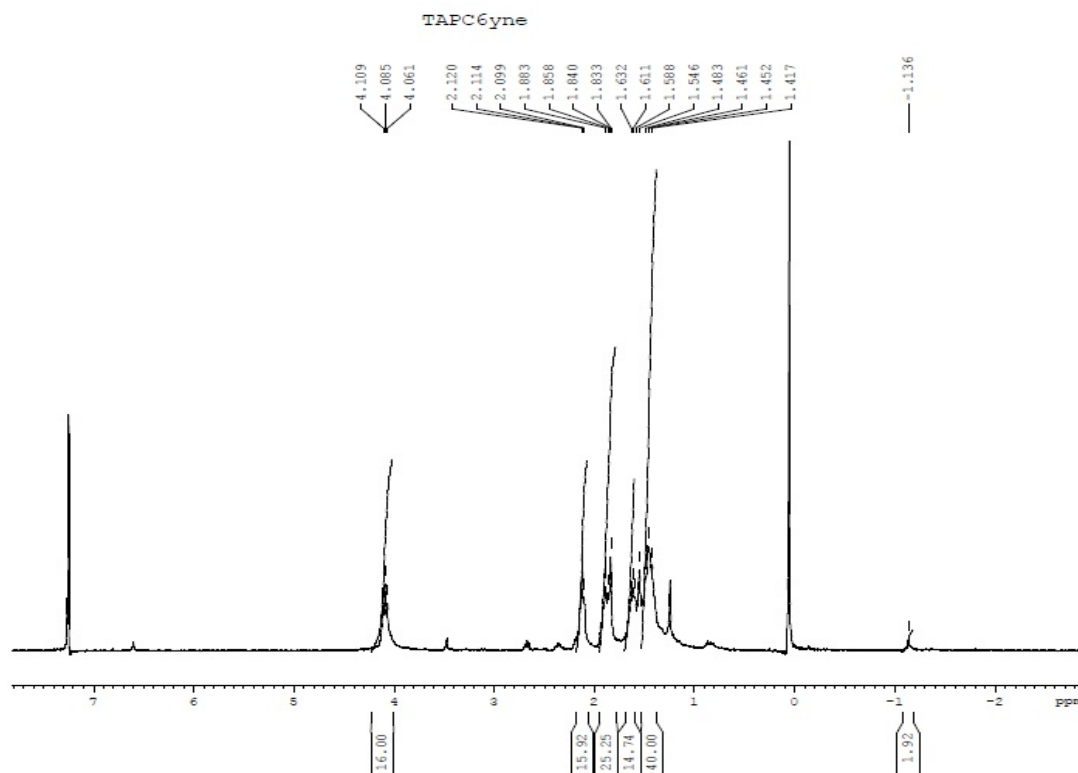


Figure S9: $^1\text{H-NMR}$ of **7b** in CDCl_3 .

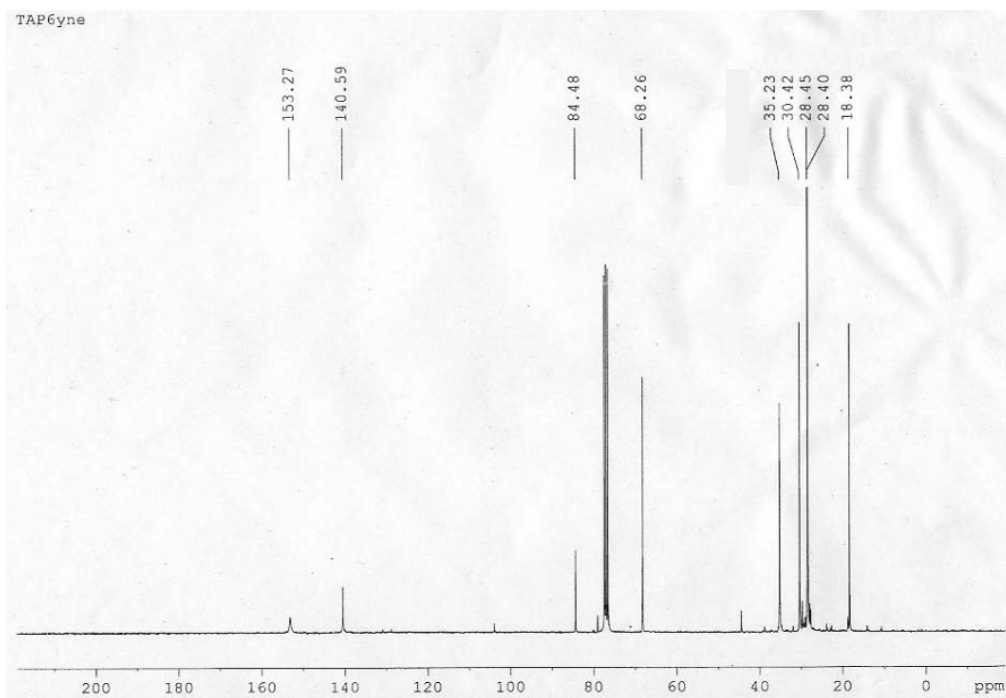


Figure S10: $^{13}\text{C-NMR}$ of **7b** in CDCl_3 .

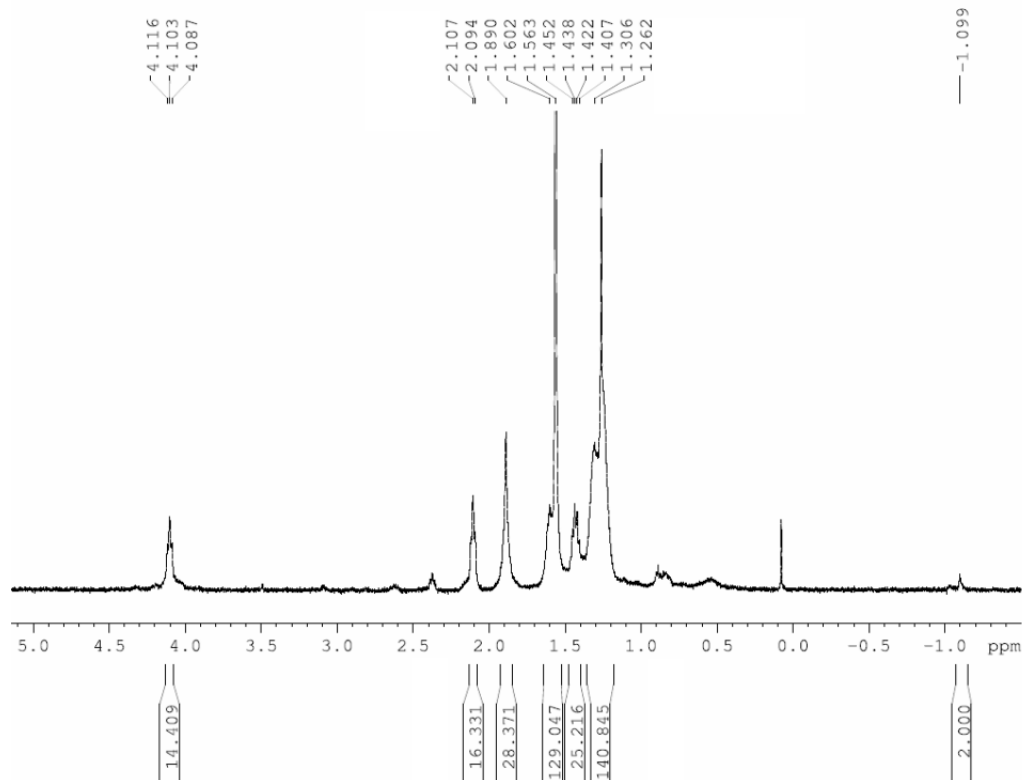


Figure S11: ¹H-NMR of 7c in CDCl₃.

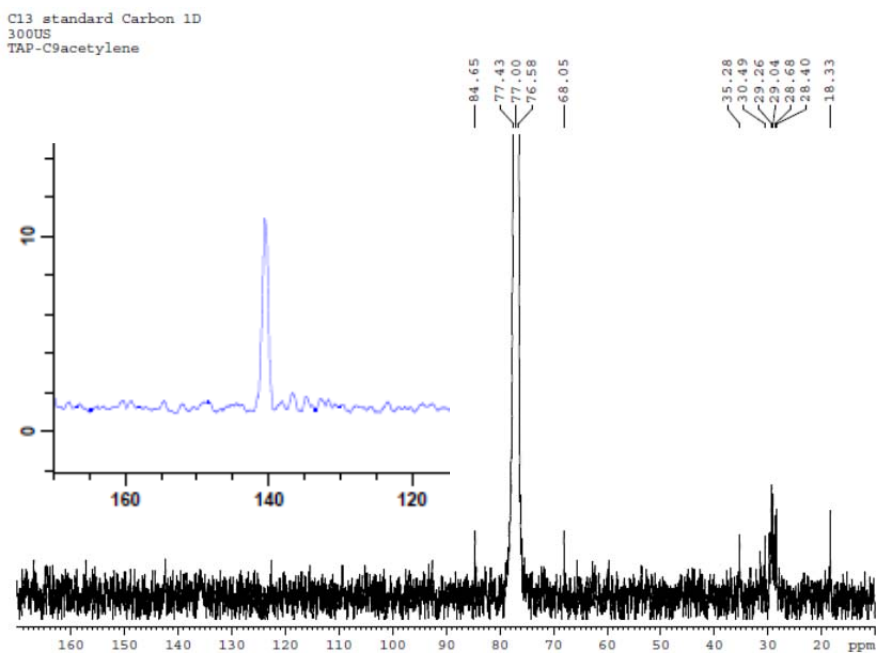


Figure S12: ¹³C-NMR of 7c in CDCl₃. The carbon signals of the TAP core were not resolved by conventional C-NMR after 36 hours of scanning. A peak for the carbon of the TAP core closer to the CH₂ group was observed by a HMBC 2D-NMR experiment at 125 MHz.

2 Mesomorphism

Instrumentation

Polarized light microscopy was performed on an Olympus TPM51 polarized light microscope that is equipped with a Linkam variable temperature stage HCS410 and digital photographic imaging system (DITO1). Calorimetric studies were conducted on a Mettler Toledo DSC 822^e and thermal gravimetric analysis was performed on a Mettler Toledo TGA SDTA 851e. Helium (99.99%) was used to purge the system at a flow rate of 60 mL/min. Samples were held at 30 °C for 30 min before heated to 550 °C at a rate of 5 °C/min. All samples were run in aluminium crucibles. XRD measurements were run on a Bruker D8 Discover diffractometer equipped with a Hi-Star area detector and GADDS software package. The tube is operated at 40 kV and 40 mA and CuK α 1 radiation ($\lambda=1.54187$ Å) with an initial beam diameter of 0.5 mm is used. A modified Instec hot & cold stage HCS 402 operated *via* controllers STC 200 and LN2-P (for below ambient temperatures) was used for variable temperature XRD measurements.

Thermal Gravimetric Analysis

Table S1: Extrapolated onset temperatures taken from 1st derivative curves and temperatures at which 0.3% weight loss has occurred.

	6a	6aCu	6b	6bCu	6c	6cCu	7a	7aCu	7b	7bCu	7c	7cCu
onset	128	117	181	139	149	140	175	150	151	141	149	142
0.3%	133	136	185	153	154	153	181	165	160	153	162	149

Differential Scanning Calorimetry (DSC)

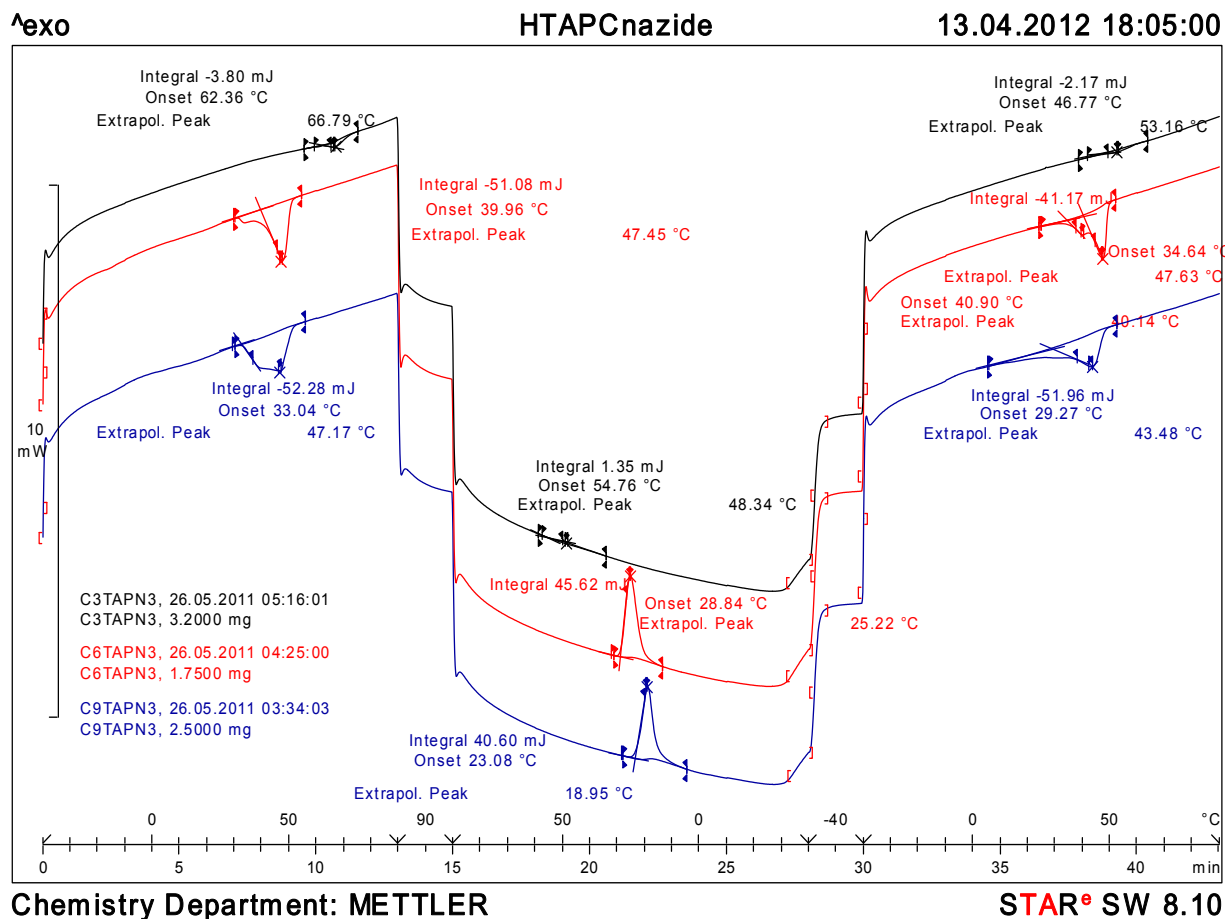


Figure S13: DSC graphs and analysis of **6a** (black), **6b** (red), and **6c** (blew) at 10 °C/min under N₂. No mesophases were observed.

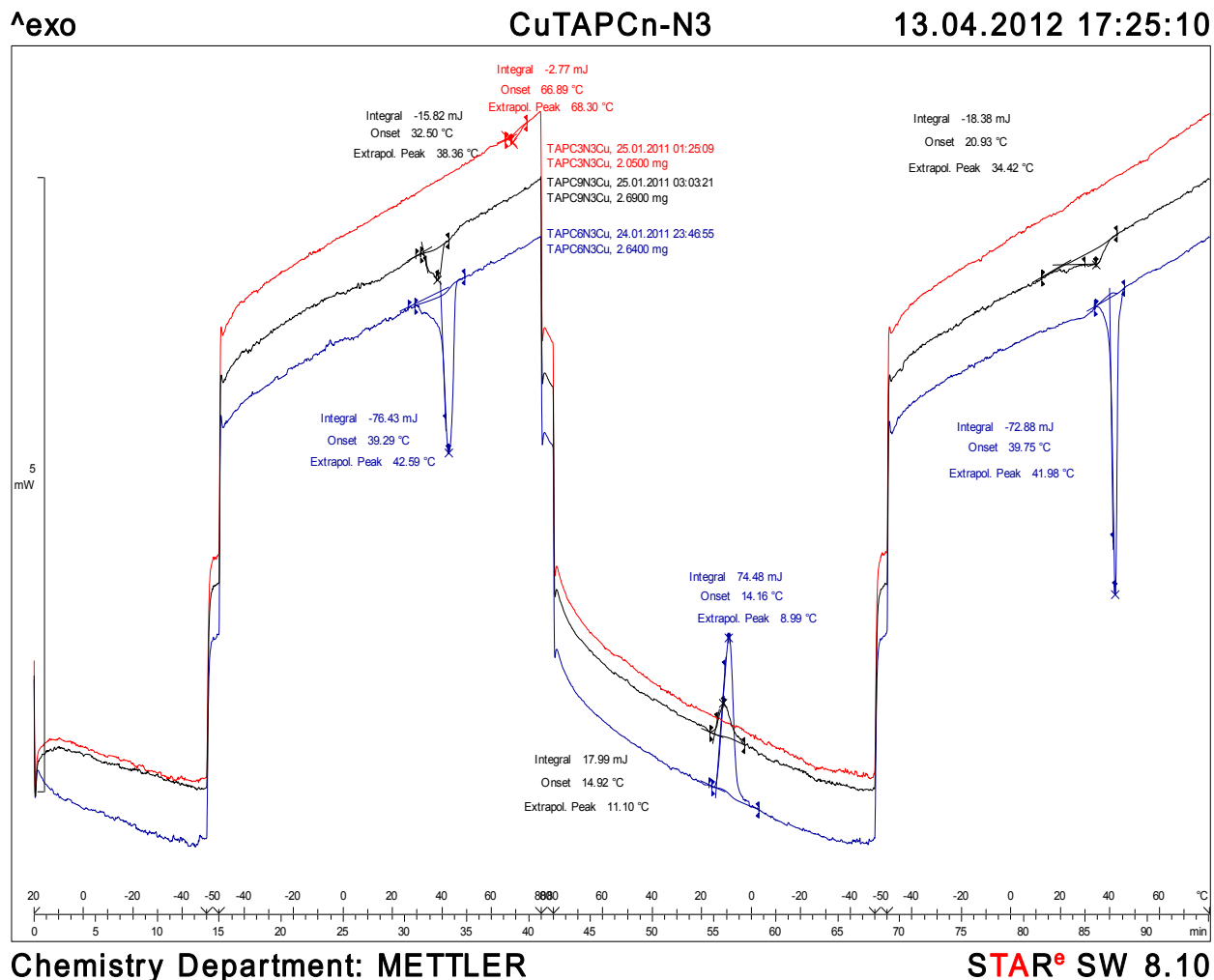
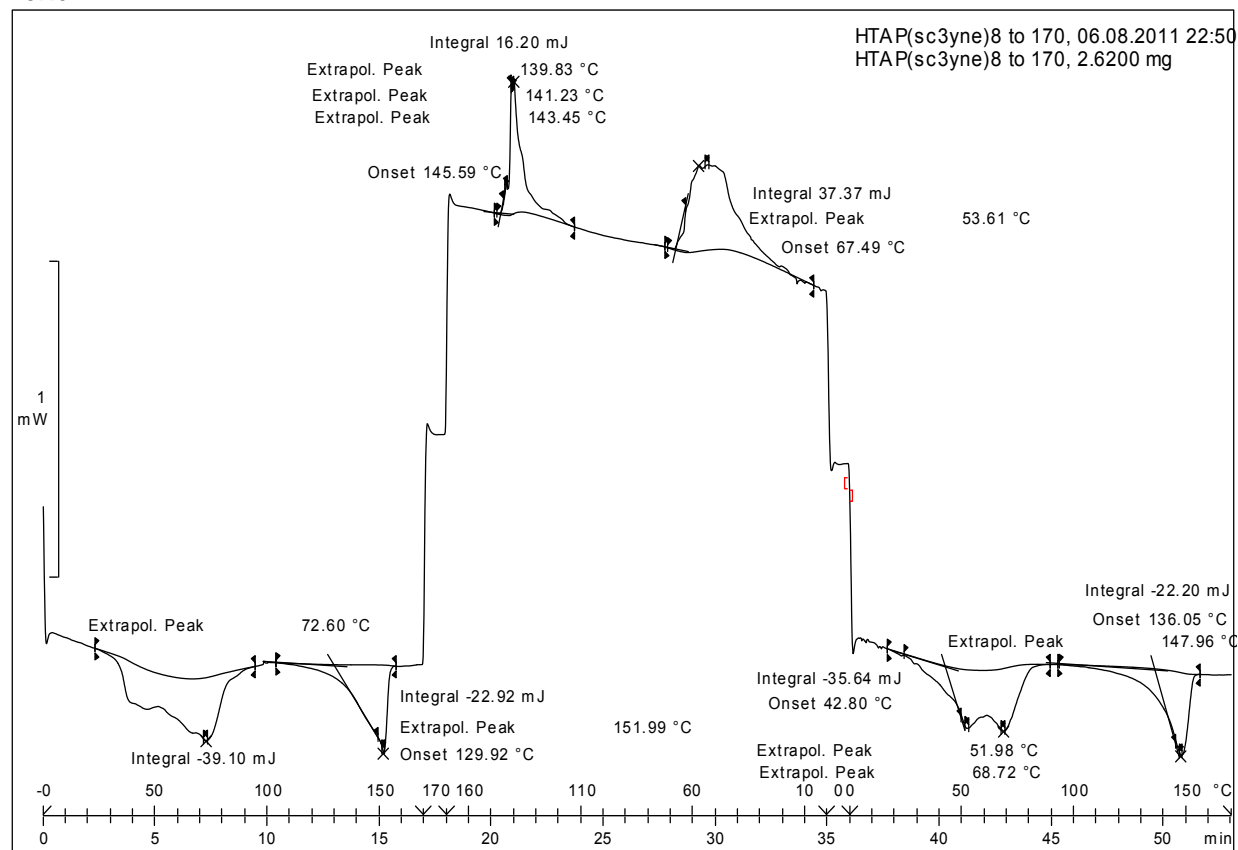


Figure S14: DSC graphs and analysis of **6aCu** (red), **6bCu** (blew), and **6cCu** (black) at 10 °C/min under N₂. Compounds **6aCu** and **6bCu** display Col_h mesophases but the clearing temperature of **6aCu** is larger than its onset of decomposition at 117 °C and the clearing transition of **6bCu** is not observed by DSC.

^exo

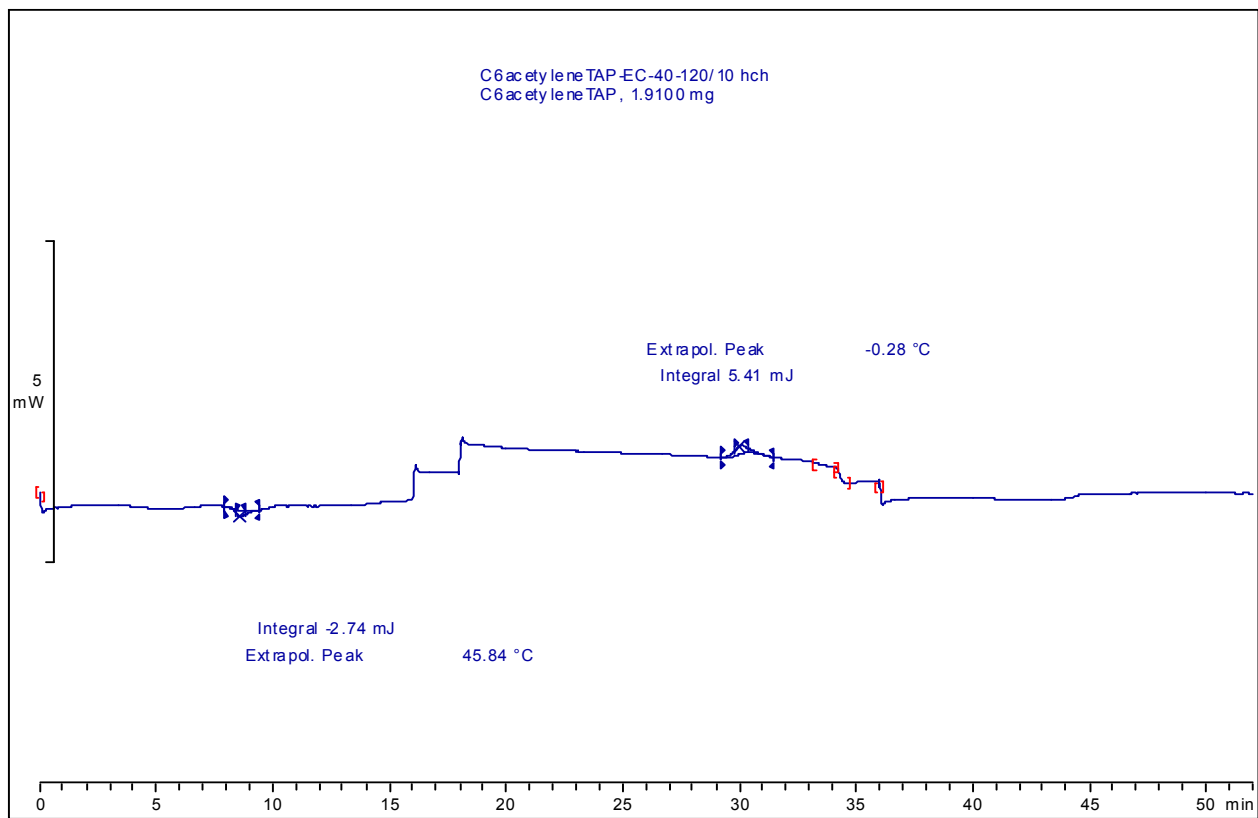


Chemistry Department: METTLER

STAR® SW 8.10

Figure S15: DSC graph and analysis of **7a** at 10 °C/min under N₂.

^exo



Chemistry Department: METTLER

STAR® SW 8.10

Figure S16: DSC graph and analysis of **7b** at 10 °C/min under N₂.

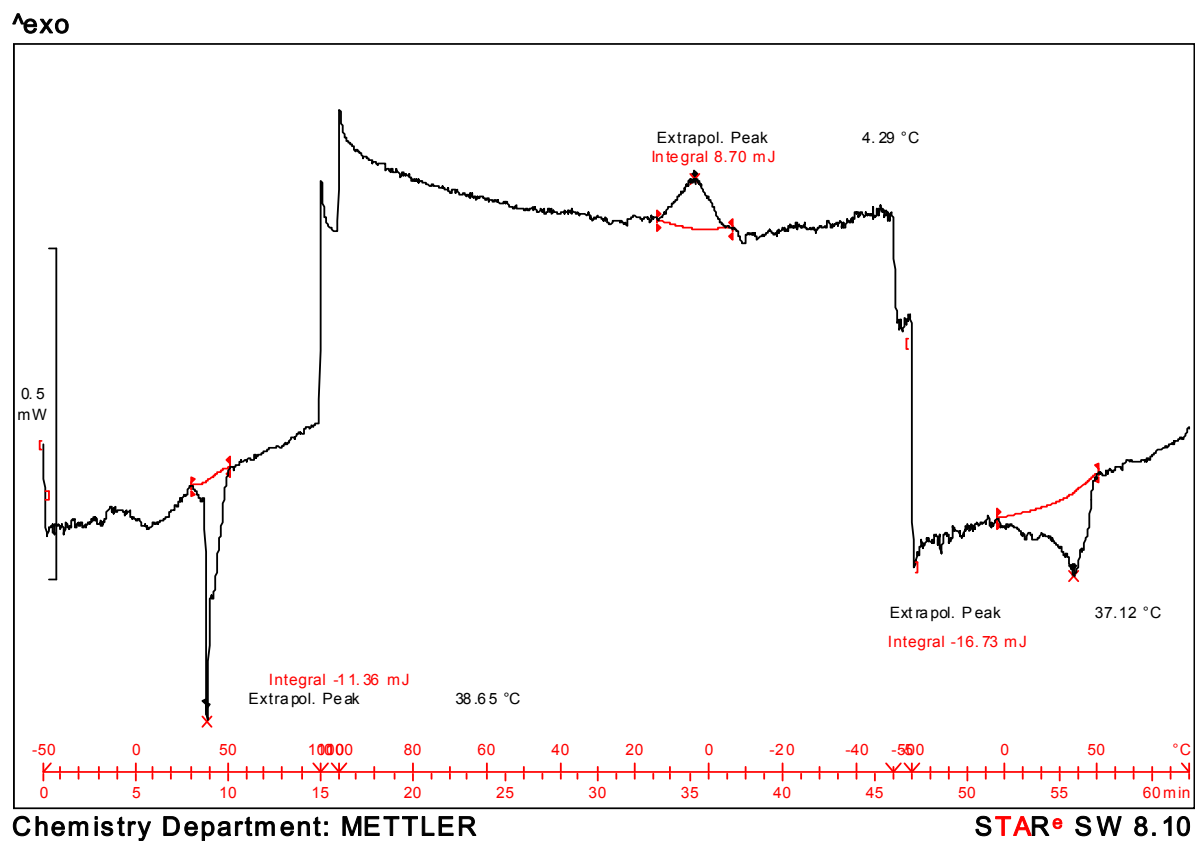
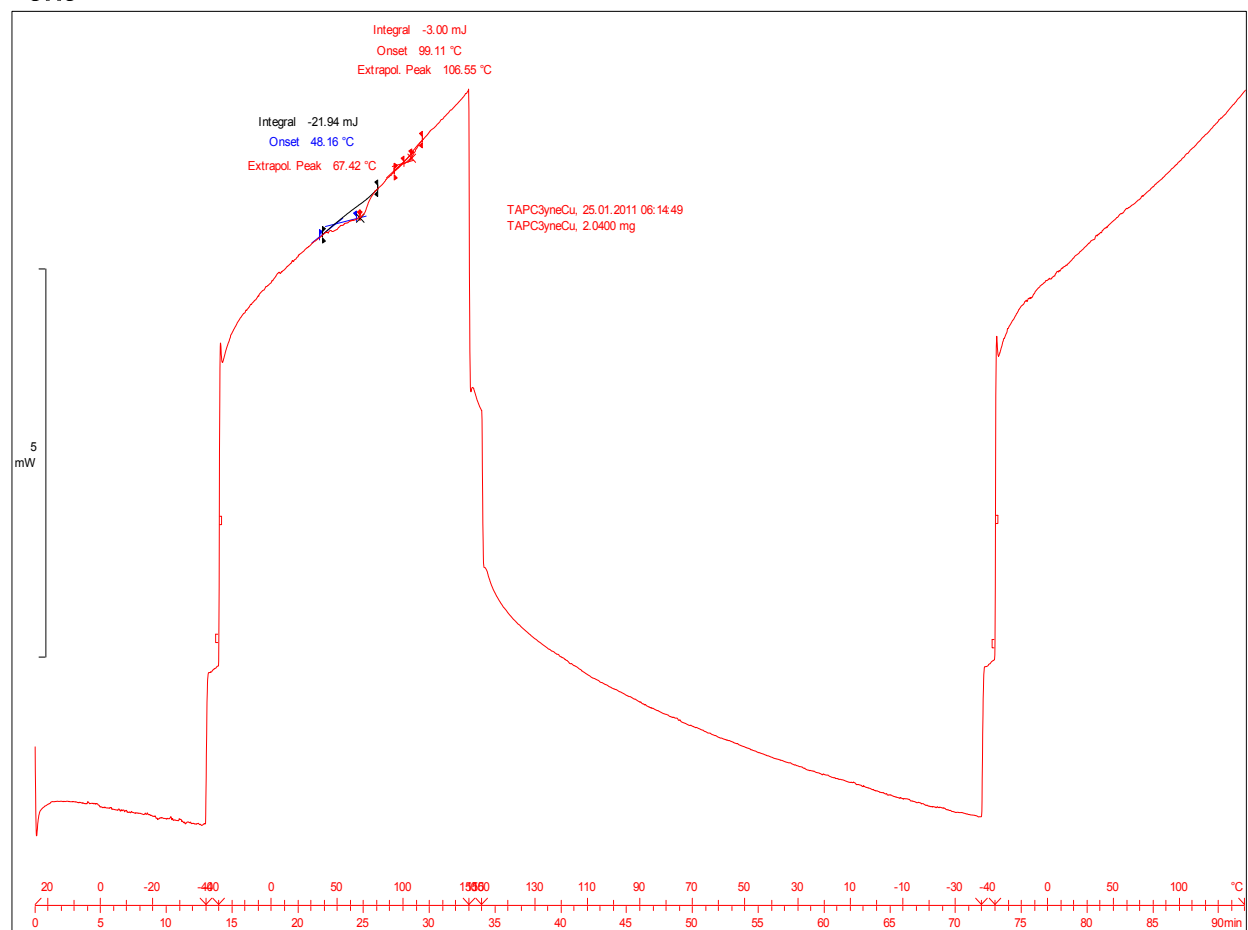


Figure S17: DSC graph and analysis of **7c** at 10 °C/min (heating) and 5 °C/min (cooling) under N₂.

Δ exo



Chemistry Department: METTLER

STAR^e SW 8.10

Figure S18: DSC graph and analysis of **7aCu** at 10 °C/min (heating) and 5 °C/min (cooling) under N₂. Melting and clearing transition are observed only in the first heating run. They reoccur if the sample is left at room temperature for 3 days.

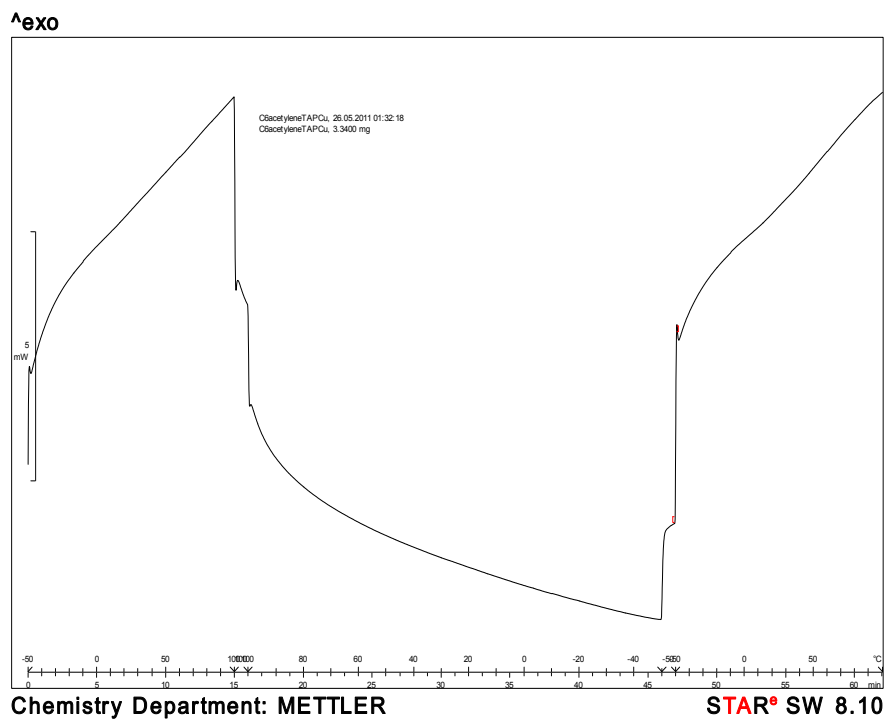


Figure S19: DSC graph of **7bCu** at 10 °C/min (heating) and 5 °C/min (cooling) under N₂. No transitions are observed.

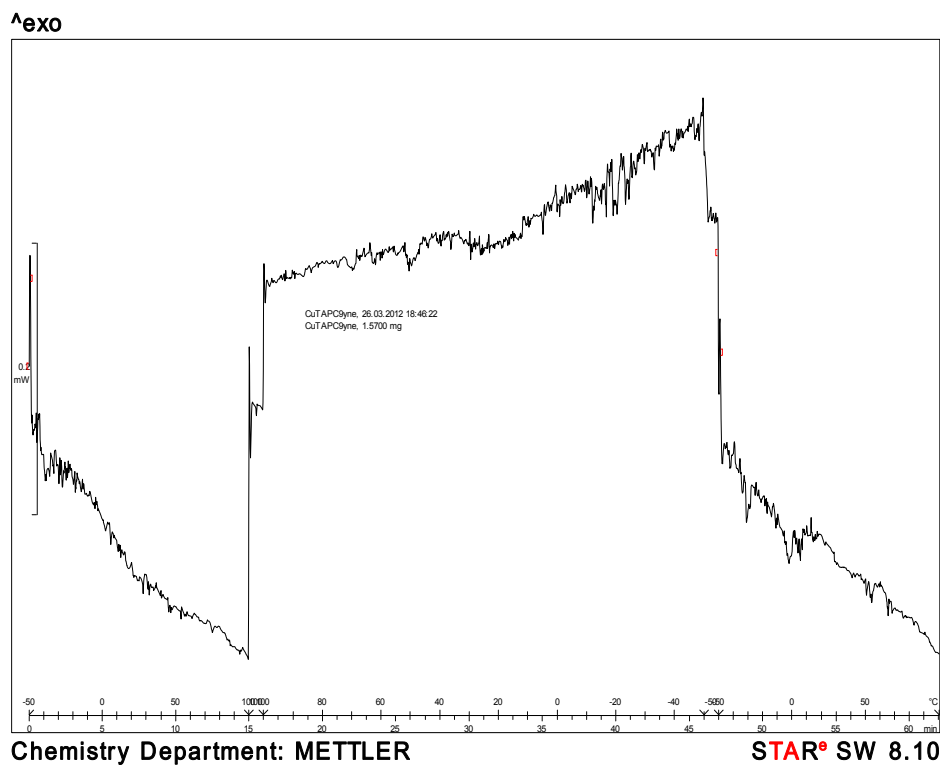


Figure S20: DSC graph of **7cCu** at 10 °C/min (heating) and 5 °C/min (cooling) under N₂. No transitions are observed.

Powder X-ray Diffraction (XRD)

CuTAP(sc3N3)8

Frame: CuTAP(sc3N3)8,25C_00

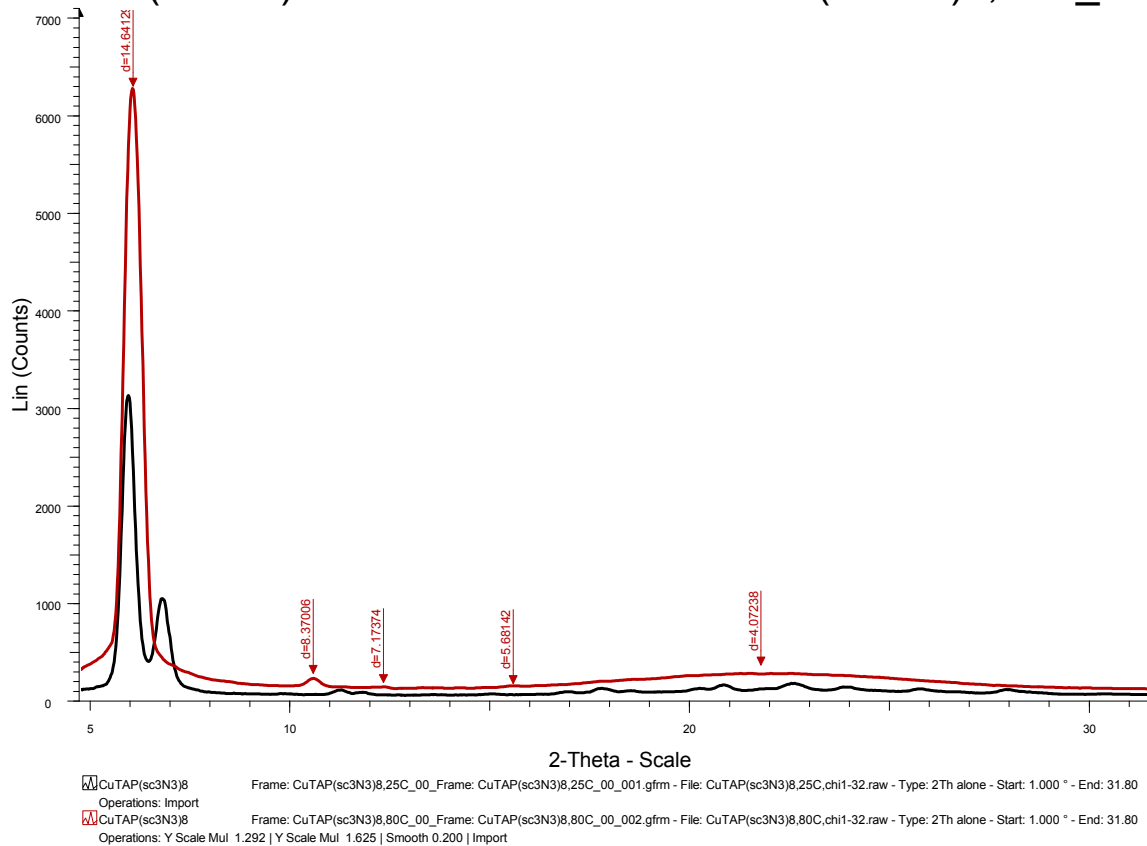


Figure S21: pXRD graphs of **6aCu** at 25 °C (black line, crystalline phase) and 80 °C (red line, Col_h mesophase).

Angle 2-theta at 80 °C	d in Å	Intensity in counts	Relative intensity in %	Calculated d values for Col _h	Assignment
6.031	14.64	5100	100	14.64	(10)
10.567	8.37	181	3.5	8.45	(11)
12.324	7.18	101	2	7.32	(20)
15.577	5.68	110	2.2	5.53	(21)
21.798	4.07	226	4.4		halo of aliphatic chains

Lattice parameter a = 16.90 Å

CuTAP(sc6N3)8

Frame: CuTAP(sc6N3)8,21C_00

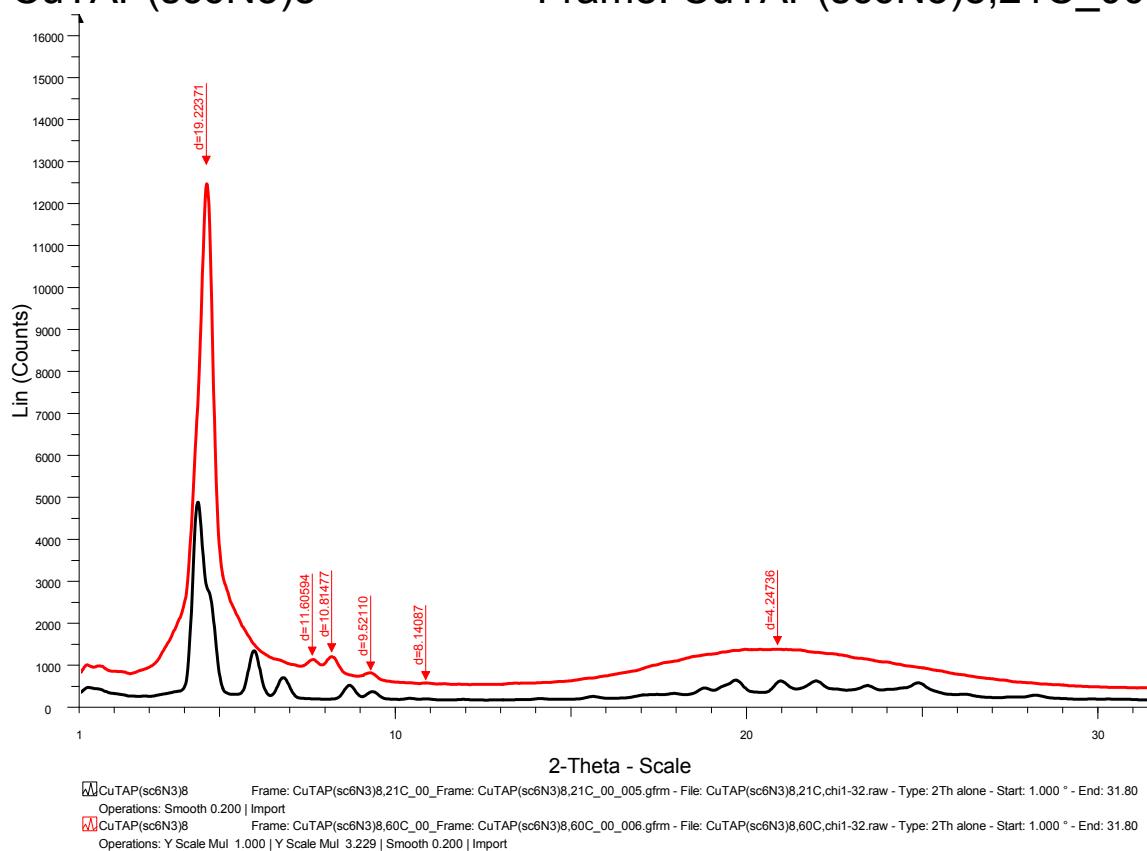


Figure S22: pXRD graphs of **6bCu** at 21 °C (black line, crystalline phase) and 60 °C (red line, Col mesophase). The reflections as assigned do not agree with a Col_h mesophase and a closer look at the shape of the small angle reflection at 19.22 Å reveals two reflections as it has a shoulder towards smaller angles. The peak positions of the two reflections are estimated to 20.415 Å and 18.981 Å.

Angle 2-theta at 60 °C	d in Å	Intensity in counts	Relative intensity in %	Calculated d values for Col _r	Assignment
4.593	19.223	12974	100	19.22	two reflections
	20.415			20.415	(11)
	18.981			18.981	(20)
7.611	11.605	1202	9.3	11.21	(31)
8.169	10.814	1281	9.9	10.21	(22)
9.281	9.521	849	6.5	9.49	(40)
10.859	8.140	617	4.8	7.89	(13)
20.897	4.247	1455	11.2		halo of aliphatic chains

Lattice parameters based on assumed Col_r mesophase a = 37.96 Å and b = 24.21.

HTAP(sc3yne)8

Frame: HTAPsc3yne,25C_00_00

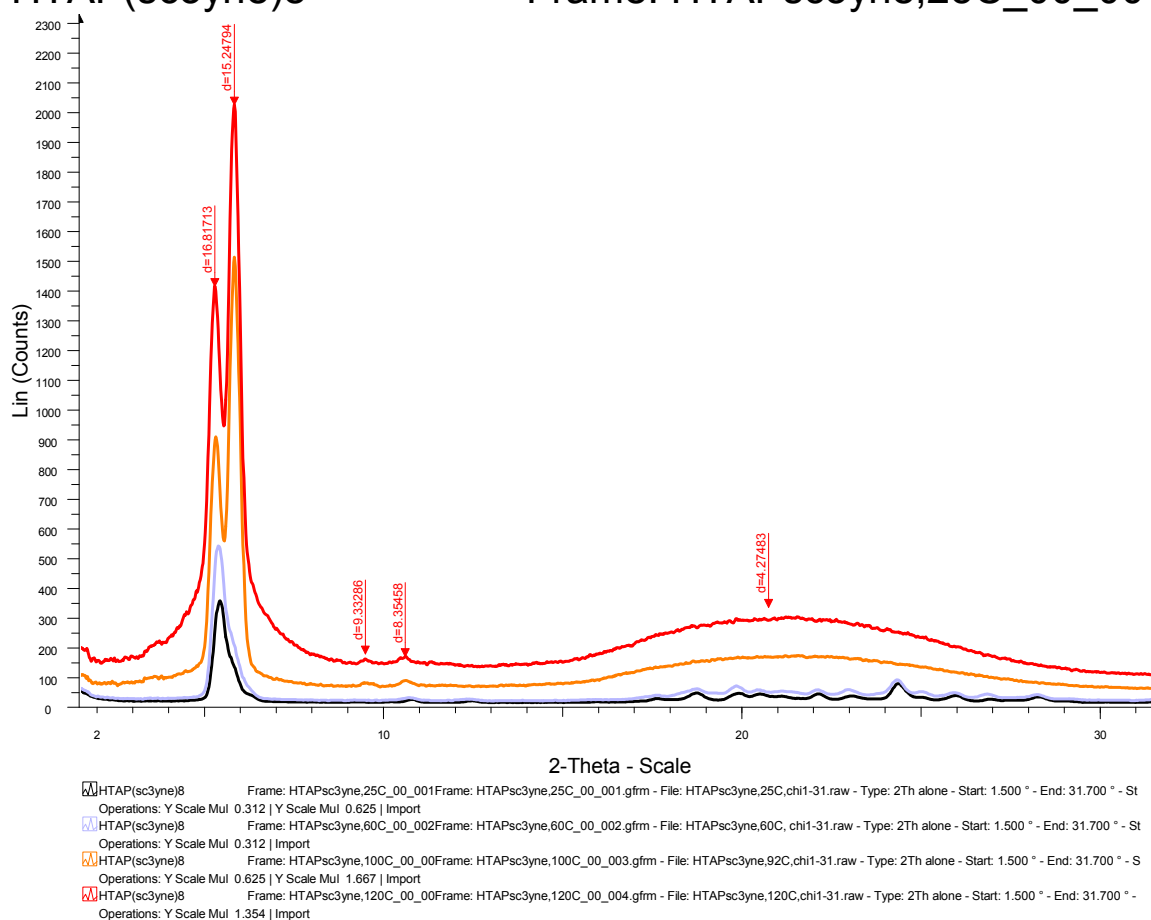


Figure S23: pXRD graphs of the crystalline phase of **7a** at 25 °C (black) and 60 °C (purple) and of its Col_r mesophase at 100 °C (orange) and 120 °C (red).

Angle 2-theta at 120 °C	d in Å	Intensity in counts	Relative intensity in %	Calculated d values for Col _r	Assignment
5.251	16.817	1415	69.8	16.817	(20)
5.791	15.248	2029	100	15.248	(11)
9.468	9.333	174	8.6	9.377	(31)
10.58	8.355	165	8.1	8.408	(40)
20.762	4.275	331	16.3		halo of aliphatic chains

Lattice parameters a = 33.634 Å and b = 17.107

CuTAP(SCn-yne)8

Frame: CuTAP(SCn-yne)8,25C

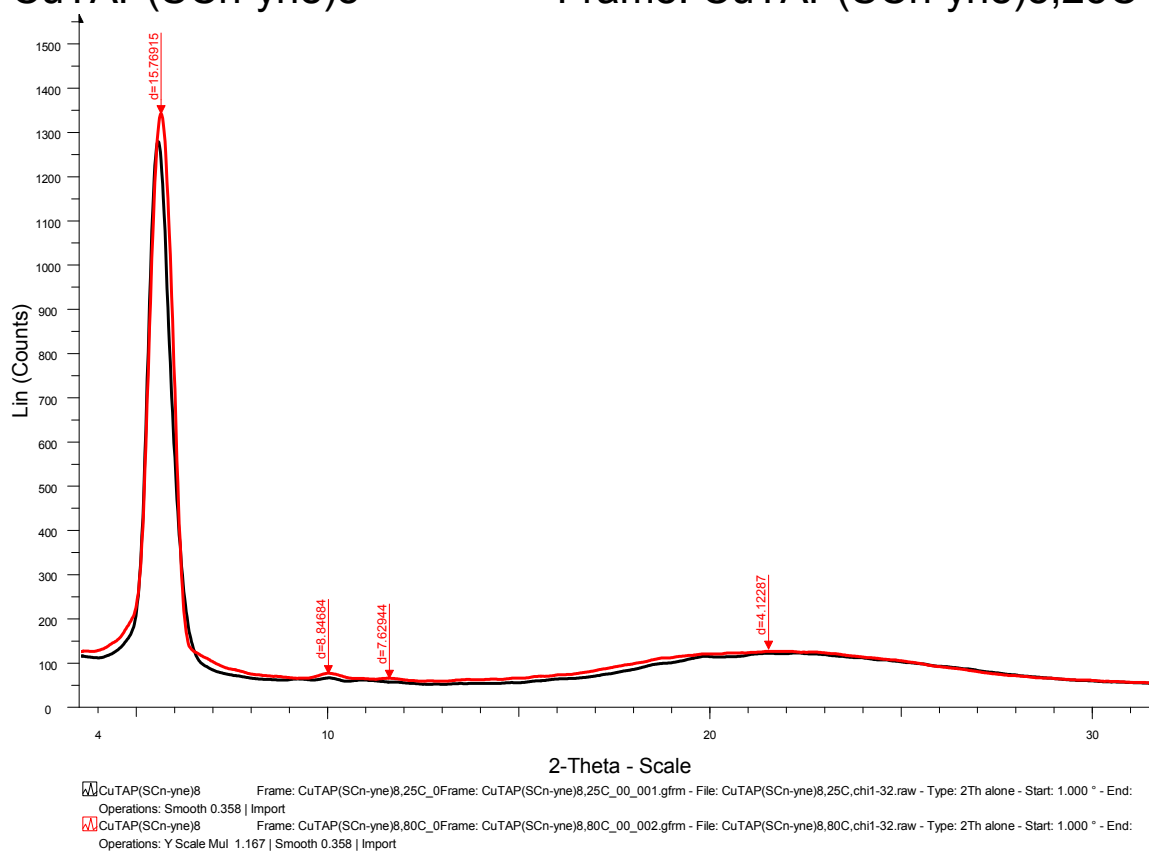


Figure S24: pXRD graphs of the crystalline phase of **7aCu** at 25 °C (black) and of its Col_h mesophase at 80 °C (red).

Angle 2-theta at 80 °C	d in Å	Intensity in counts	Relative intensity in %	Calculated d values for Col _h	Assignment
5.6	15.769	1344	100	15.77	(10)
9.99	8.847	72	5.4	9.10	(11)
11.589	7.629	61.8	4.6	7.88	(20)
21.536	4.123	128	9.5		halo of aliphatic chains

Lattice parameter a = 18.21 Å

Polarized Optical Microscopy (POM)

All images are 220 x 220 μm large and were taken with crossed polarizers.

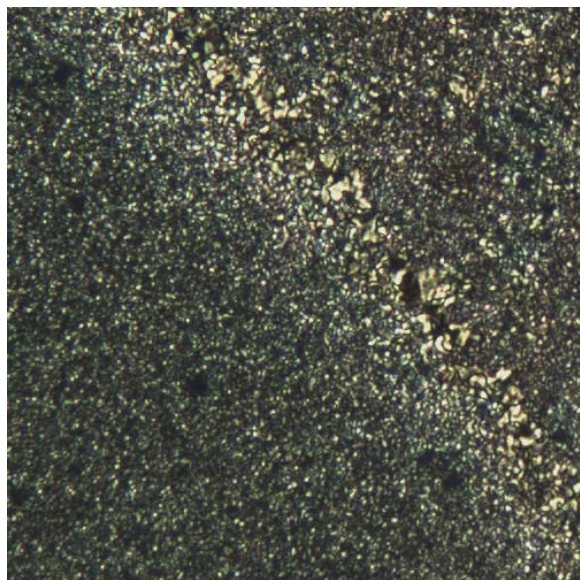


Figure S25: POM micrograph of **6aCu** between glass slides at 100 $^{\circ}\text{C}$ (200x). The domain size is small but some areas of fan-shaped textures are observed that are characteristic for columnar mesophases.



Figure S26: POM micrographs of **6bCu** as a thin film on glass at 41 $^{\circ}\text{C}$ (left) and 45 $^{\circ}\text{C}$ (right) on cooling from the isotropic liquid (200x). The dendritic growth textures are typical for Col_h and Col_r mesophases. Dark areas are free of compound due to local dewetting of the thin film (about 500 nm thick).

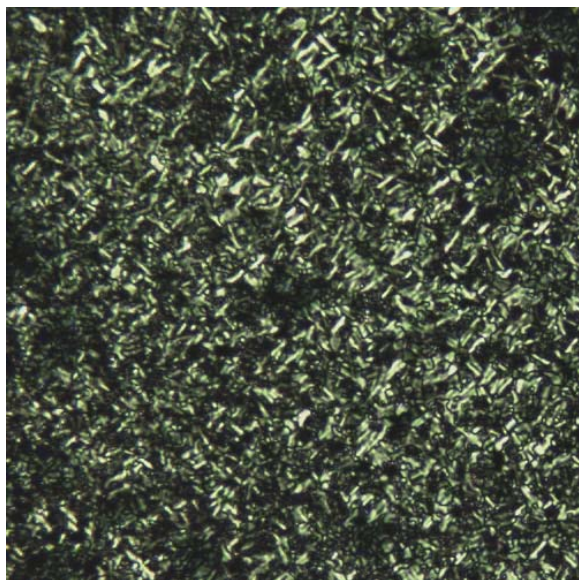


Figure S27: POM micrograph of **7a** as a thin film on glass at 120 °C on cooling from the isotropic liquid (200x). The observed fan-shaped texture is characteristic for columnar mesophases.

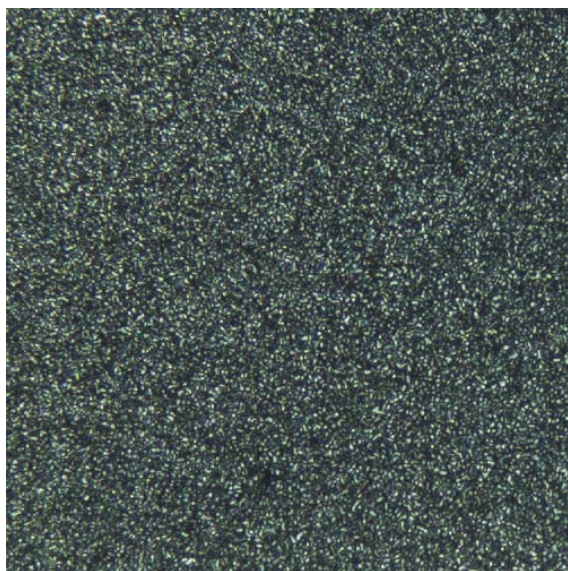


Figure S28: POM micrograph of **7aCu** between glass slides at 100 °C (200x). The domain size is very small and the resulting texture is not characteristic for a specific type of mesophase.

3 Cross-Linking in solution and Col_h Mesophase

For the cross-linking in solution equal molar amounts (1:1 mixture) of for example **6a** (45 mg, 0.04 mmol) and **7a** (50 mg, 0.04 mmol) were dissolved in 50 mL DMF. Copper (II) acetate (64 mg, 0.32 mmol) and sodium ascorbate (190 mg, 0.96 mmol) were added under N₂ atmosphere and the reaction mixture was stirring at 50 °C for 2 hrs. The reaction mixture was filtered at room temperature and washed with MeOH (2 x 50 mL) and water (2 x 50 mL). The dark flaky solid was dried *in vacuo* to yield the cross-linked insoluble product in 91.5% (87 mg).

For the cross-linking in the Col_h mesophase equal molar amounts (1:1 mixture) of **6aCu** and **7aCu** were dissolved in ethyl acetate and then dried in high vacuum at room temperature. All mixtures were studied within an hour of their initial mixing.

[^]exo

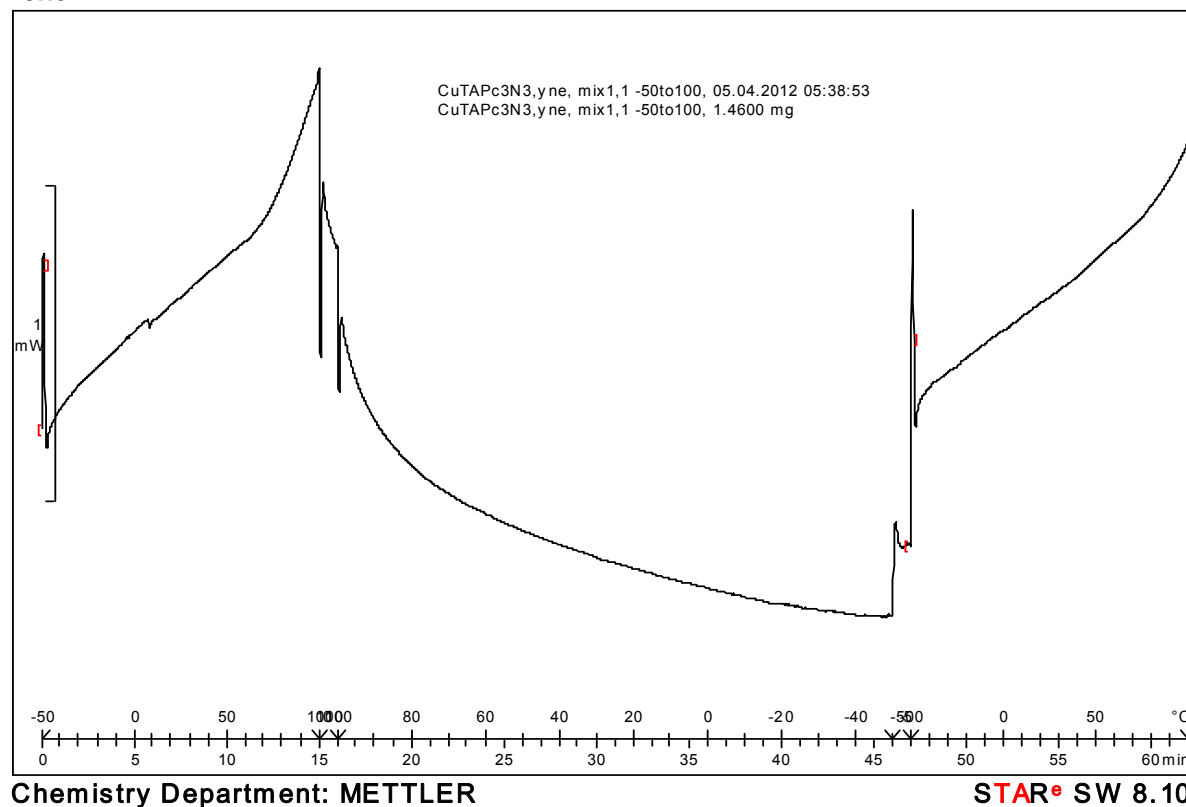


Figure S29: Low temperature DSC (10 °C/min, N₂) of a freshly prepared 1:1 (mol/mol) mixture of **6aCu** and **7aCu**. No phase transitions are observed but the baseline rises exothermally, especially at temperatures above 80 °C, which is attributed to the exothermic click reaction.

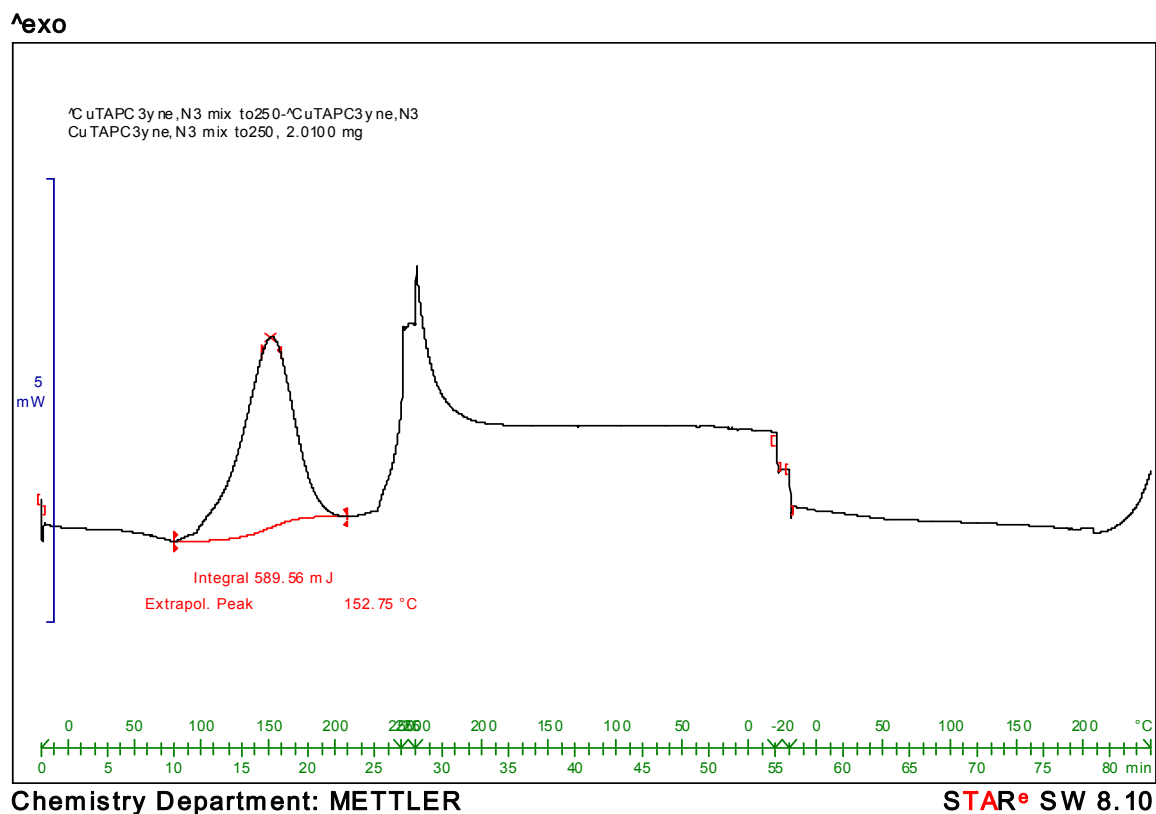


Figure S30: High temperature DSC (10 °C/min, N₂, baseline subtracted) of a freshly prepared 1:1 (mol/mol) mixture of **6aCu** and **7aCu**. The large exothermic peak (293 J/g) is attributed to the exothermic click reaction. The rise of the baseline above 200 °C is likely caused by thermal decomposition.

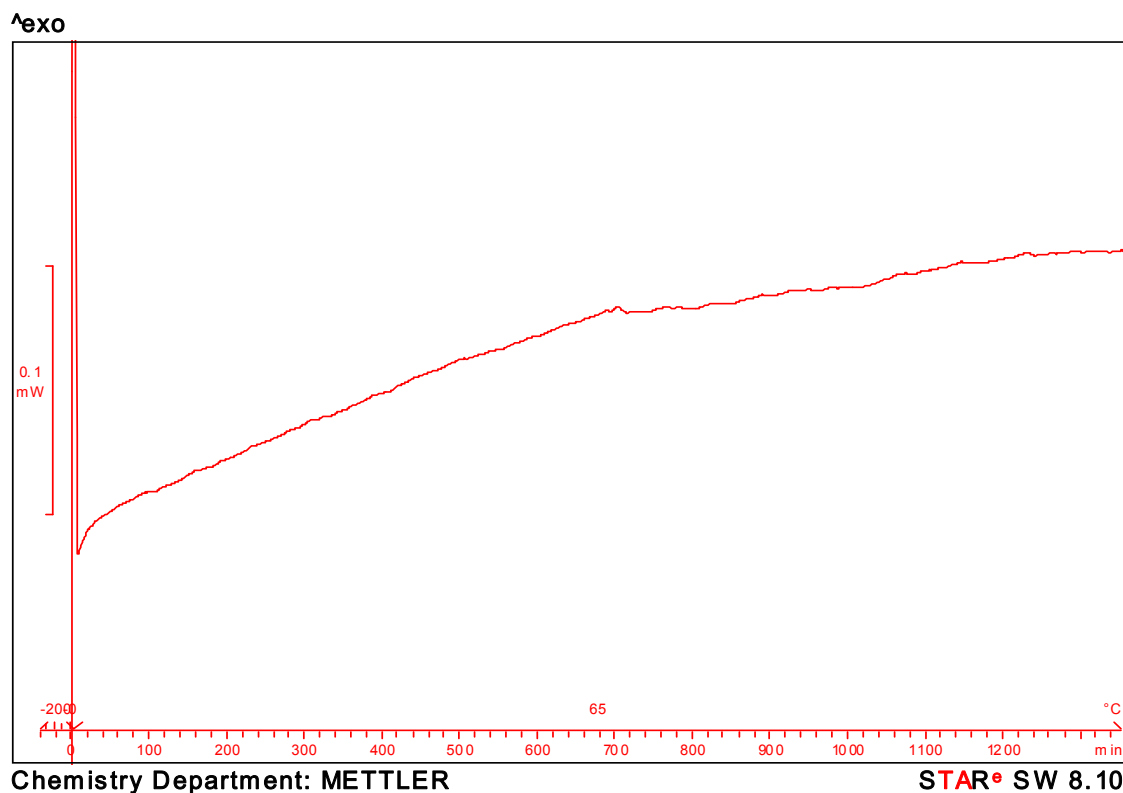


Figure S31: Isothermal DSC run (heated to 65 °C at 10 °C/min and then isothermal for 2 days, N₂) of a freshly prepared 1:1 (mol/mol) mixture of **6aCu** and **7aCu**. The positive slope of the curve is attributed to the exothermic click reaction. Progress of the reaction appears to be faster in the first 700 minutes (steeper slope) and then gradually slowing down until it is almost zero after about 1300 minutes (22 hours).

4 Langmuir and Langmuir-Blodgett Films

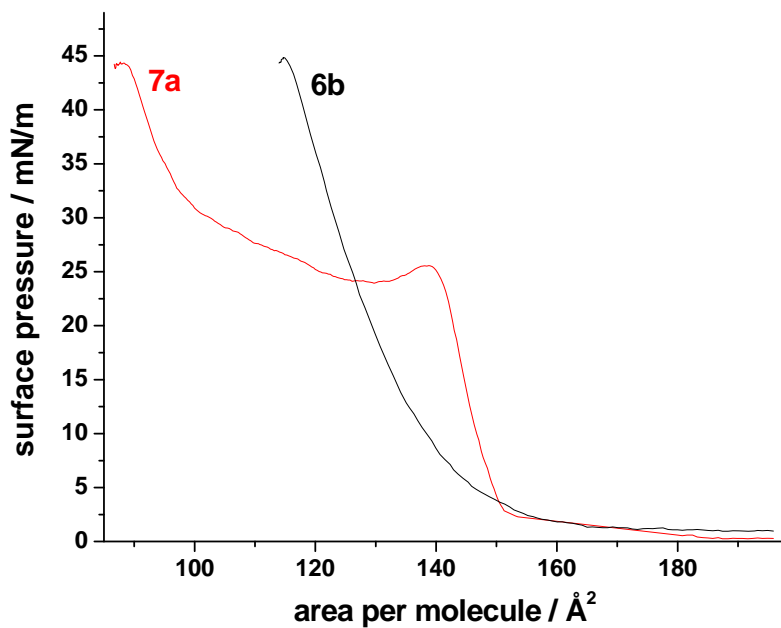


Fig. S32 Surface pressure area isotherms of TAPs **6b** and **7a** on pure water at pH = 6.5 and 25 °C.

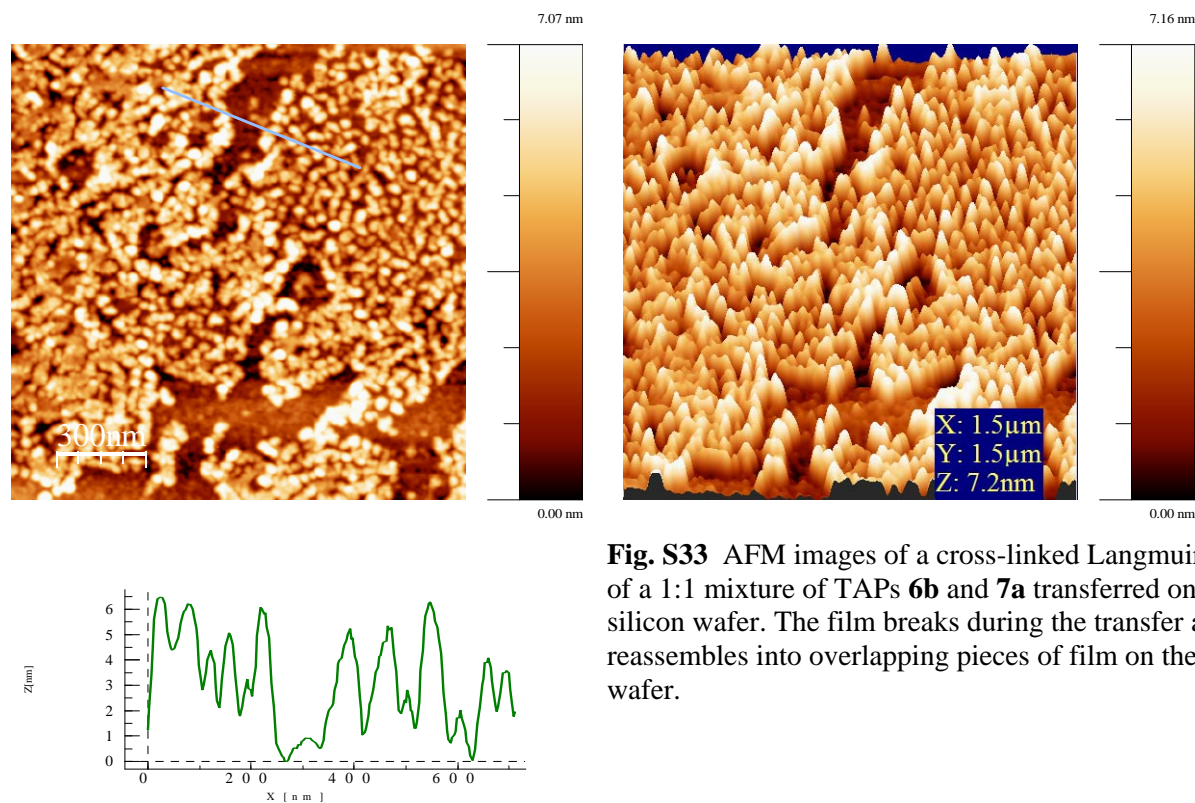


Fig. S33 AFM images of a cross-linked Langmuir film of a 1:1 mixture of TAPs **6b** and **7a** transferred onto silicon wafer. The film breaks during the transfer and reassembles into overlapping pieces of film on the wafer.